Pacific Upwelling and Mixing Physics: A Science and Implementation Plan

W.S. Kessler
J.N. Moum
M.F. Cronin
P.S. Schopf
D.L. Rudnick
L. Thompson

May 2004

Contents

Summary 1
1. Rationale 2
2. Scientific Background 7
2.1 Upwelling 7
2.2 Turbulent mixing 11
2.3 Heat fluxes 16
2.4 Frontal processes 17
2.5 Ocean-atmosphere feedbacks 21
2.6 Gaps in our understanding of the processes that modulate equatorial SST 22
3. Implementation of PUMP 24
3.1 Objectives of the PUMP field program 24
3.2 PUMP components 26
3.2.1 Historical data analysis 26
3.2.2 Time series: Seasonal and interannual variability across the cold tongue 27
3.2.3 IOPs: Rapid/reduced cooling experiments 32
3.2.4 Modeling 35
3.3 Relation with other programs 39
3.4 Budget and timeline 41
4. Acknowledgments 42
References 43

List of Figures

1 Annual cycle of SST at 0°, 140°W 3
2 Nino3 amplitude vs. ocean model diffusivity 5
3 Schematic processes targeted by PUMP 7
4 Section of meridional velocity (cm s^{-1}) averaged over 170°W–95°W 9
5 Mean (1993–96) profiles of vertical velocity and transport (integrated over 5°S–5°N, 155°W–95°W) 10
6 Mean vertical-meridional circulation at 140°W in the MOM2 model 11
7 Turbulence dissipation rate ϵ for 10 days of the Tropical Instability Wave Experiment (TIWE) in 1991 13
8 Turbulent heat and momentum flux profiles at 0°, 140°W. 14
9 Atmospheric and oceanic conditions across a sharp front in a detailed meridional section along 95°W during EPIC 2001 19
10 Example of the sensitivity of winds to SST 20
11 Meridional decorrelation of meridional velocity along 140°W from 2°S to 2°N 30
12 Schematic moored array for PUMP 31
13 Timeline of PUMP Intensive Observation Periods (two IOPs, during July and November–December) 34
14 Timeline of PUMP showing the elements described in section 3.2. . . 42

Summary

The Pacific Upwelling and Mixing Physics (PUMP) experiment is a process study designed to improve our understanding of the complex of mechanisms that connect the thermocline to the surface in the equatorial Pacific cold tongue. Its goal is to observe and understand the interaction of upwelling and mixing with each other and with the larger-scale equatorial current system. Its premises are, first, that the least understood contributions to the modulation of equatorial SST are upwelling and mixing, and second, that climate-scale ocean models are now ready to exploit realistic vertical exchange processes, but need adequate observational guidance.

The outcome of PUMP will be advancements in our ability to diagnose and model both the mean state of the coupled climate system in the tropics and its interannual and interdecadal variability.

The primary objectives of this program are:

1. To observe and understand the 3D time evolution of the near-equatorial meridional circulation cell under varying winds, sufficiently well to serve (a) as background for the mixing observations in objective 2; (b) as a challenge to model representations.

2. To observe and understand the mixing mechanisms that determine (a) the depth of penetration of wind-input momentum and the factors that cause it to vary; (b) the transmission of surface heat fluxes into the upper thermocline and the maintenance of the thermal structure in the presence of meters per day upwelling.

3. To observe and understand the processes that allow and control exchange across the sharp SST front north of the cold tongue, including both small-scale frontal dynamics and the effects of tropical instability waves.

To achieve these objectives requires a concerted effort with four interlocking components:

1. An integrated reanalysis of historical data should be undertaken with the specific goals of providing both experimental guidance and, by producing uniform data sets, expanding the range of climate states for further model diagnosis.

2. A multi-scale and coordinated modeling effort should be directed toward aiding the observational effort to begin with, and later toward interpreting and parameterizing observational results.

3. An extended (2–3 year) and expanded (2/3 degree spatial resolution) moored observational presence should be established along 140°W spanning the cold tongue to quantify scales of and changes in equatorial upwelling.

4. Two intensive observation periods to quantify the relative effects of upwelling and mixing within the moored observational array should be targeted to resolve the distinctions between the well-defined periods of Rapid Cooling and Reduced Cooling at 140°W, both on and just off the equator.

1. Rationale

The role of the oceans in climate is largely centered around the transport and storage of heat. Regions of strong divergence in ocean heat transport are reflected in high net surface heat flux; among these, the Pacific equatorial cold tongue is one of the most persistent and intense regions of ocean heat gain. This narrow strip of high ocean heat uptake is important not only for the mean climate: its variability on interannual to interdecadal timescales is a key player in the global climate system, especially in the El Niño-Southern Oscillation (ENSO) phenomenon and in its decadal variation, which have global consequences.

The equatorial cold tongue complex is a region where strong upwelling occurs in the presence of vigorous turbulent mixing; the resulting intimate connection between the thermocline and the surface allows the interaction of basin-scale ocean dynamics and property transports with the equatorial atmosphere that responds sensitively to variations of SST. Here, equatorial undercurrent (EUC) water is transformed in the process of being entrained into the surface layers.

An important practical focus of the climate community over the past two decades has been the manifestation of long-term perturbations (ENSO events) to a "background state." But we do not yet understand the physical processes that are responsible for maintaining the "background state." In fact, we are just beginning to define a "background state." We now have 20 years of nearly continuous data at several locations in the equatorial Pacific from the TAO array of moorings as well as satellite records of greater spatial but lesser temporal extent. One representation of the "background" state is the annual cycle of SST constructed from the time series at 0°, 140°W (Fig. 1). By this definition, the "background state" is clearly dynamic, with strong heating and cooling cycles indicated in the mean that are consistent from year to year in both their timing and in the rates at which they occur. Even after being completely disrupted by El Niño events the normal annual cycle recovers in a few months. Presumably, this indicates a systematic and robust annual variability of the upwelling/mixing regimes. But we have no observational evidence of this (mixing observations have never been made during the boreal fall rapid cooling regime, where the effects of mixing and upwelling are most prominent). Nor do we understand what causes changes in these regimes.

Uncertainties abound: not only is the net heat transport uncertain, the details of the upwelling (how narrow, how filamentary) are poorly understood; high shears and low Richardson numbers above the EUC permit elevated diapycnal mixing of heat and momentum, but the spatial structure, intermittency and true nature of the mixing is unknown; internal wave dynamics are complicated by the location near the equator. We have little idea how this circulation spins up or down in response to varying winds. The diurnal cycle is very strong, and has been implicated in intermittent "deep cycle" turbulence that carries surface-driven mixing well below the depth of direct wind influence. The region is also high in biological activity, as upwelled water brings nutrients toward the euphotic zone, where growth

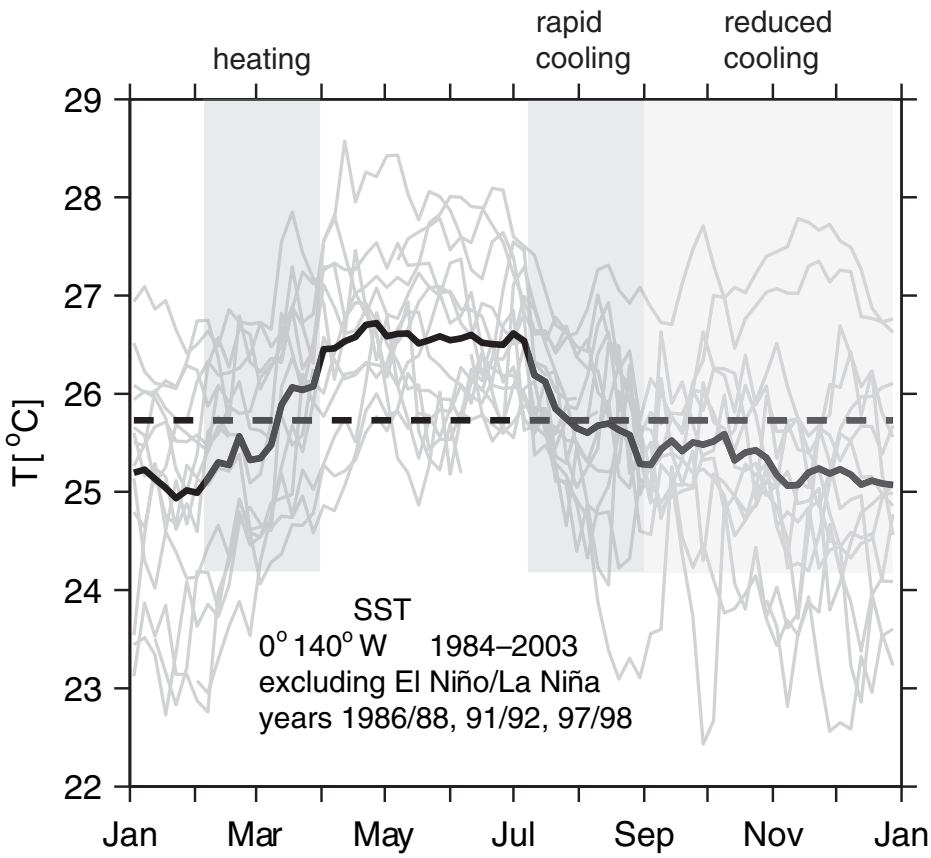

Figure 1: Annual cycle of SST at 0°, 140°W, illustrating the periods of heating and cooling during the year. Light gray lines show each individual year since 1984 overlaid (years of strong ENSO anomalies have been omitted as noted). The heavy black line shows the average annual cycle. Shading shows the months of maximum heating and maximum cooling, and a period of reduced cooling with active tropical instability wave activity, that occur consistently in almost all years.

alters the transmissivity of the water and provides an effective means for modifying the absorption of solar energy at depth. We know enough to sketch some of these processes on a schematic (see Fig. 3) but we have yet to understand how they vary either in time or as a function of distance from the equator. Perhaps most importantly, we do not understand the hierarchy of larger scale processes that act to trigger changes in the upwelling/mixing regimes.

Our understanding of the dynamics of ENSO has evolved over the past few decades to the point where numerical models have been constructed based on elegant yet simple theories, and these models have had significant success in simulating the ENSO phenomenon. Yet, these theories and models are based on perturbation analyses in which important properties of the mean state are controlled. Attempts to use fully coupled non-linear general circulation models (GCMs) to simulate and/or forecast El Niño have been less successful, unless constrained by sophisticated data assimilation tech-

niques and run for short forecast periods, over which equally sophisticated analysis techniques are used to correct for well-documented "model drift."

This model drift is essentially a reflection of the fact that the coupled GCMs produce a "climate" that is not sufficiently close to reality. There are two prominent and vexing problems that remain for the coupled GCMs: (1) the tendency within the atmosphere to form "double" or "split" representations of the intertropical convergence zone, and (2) the failure in ocean models to faithfully simulate the supply of cold subsurface waters to the cold tongue and to establish the proper profile of temperature in the upper few hundred meters of the equatorial ocean.

The failure of ocean models to accurately simulate nature is no longer a problem of bad numerics, limited resolution, or imprecise calculation. The advent of extensive supercomputing resources now allow us to simulate the tropical ocean with high resolution and high-order numerics. The largest impediment to advancing the state of tropical ocean simulation is an adequate understanding, backed by observational evidence, of the processes at work within the equatorial cold tongue. Our parameterizations of these physics is at best rudimentary, and captures only the simplest processes in a crude way. The ability to accurately simulate the realistically stratified and sheared equatorial ocean still lies ahead.

The relation between SST and thermocline depth is the key parameterization in simple ENSO models, with the memory carried in thermocline depth the dominant source of oscillation. In coupled GCMs, the oceanic vertical diffusivity is found to be a principal factor in the amplitude of their ENSO oscillations, with low background diffusivity producing a sharper thermocline and realistically more intense El Niño events (Meehl *et al.*, 2001; Fig. 2). In all these models, the essential subsurface memory is communicated to the surface through variations of either upwelling itself or the vertical temperature gradient it works on. Observations of upwelling in the context of the full three-dimensional circulation would spur advances in validating and improving this crucial and largely unexplored aspect of OGCM physics.

Previous work over two decades has made important measurements in the equatorial Pacific, including velocity and temperature profiles, a few estimates of vertical velocity w based on horizontal divergence, and three month-long mixing surveys. However, because equatorial SST variability is a convolution of surface fluxes, mixing and upwelling in a complex and time-dependent meridional circulation, these observations have not yielded an understanding of the mechanisms of vertical exchange that can be distilled into improved model parameterizations. Further, existing observations have concentrated narrowly on the equator and have not been able to provide a description of the meridional circulation that would let us evaluate the realism of these structures in OGCMs, whose development has also focused primarily on the equatorial thermocline and zonal currents. But cold tongue SST is a function of the entire structure of the circulation that feeds thermocline water to the surface, and this structure is nearly unknown. Three-dimensional velocity changes in response to varying winds depend on how the surface layer divergence is distributed in the vertical, which is controlled by the mixing that communicates wind-input momentum from the surface.

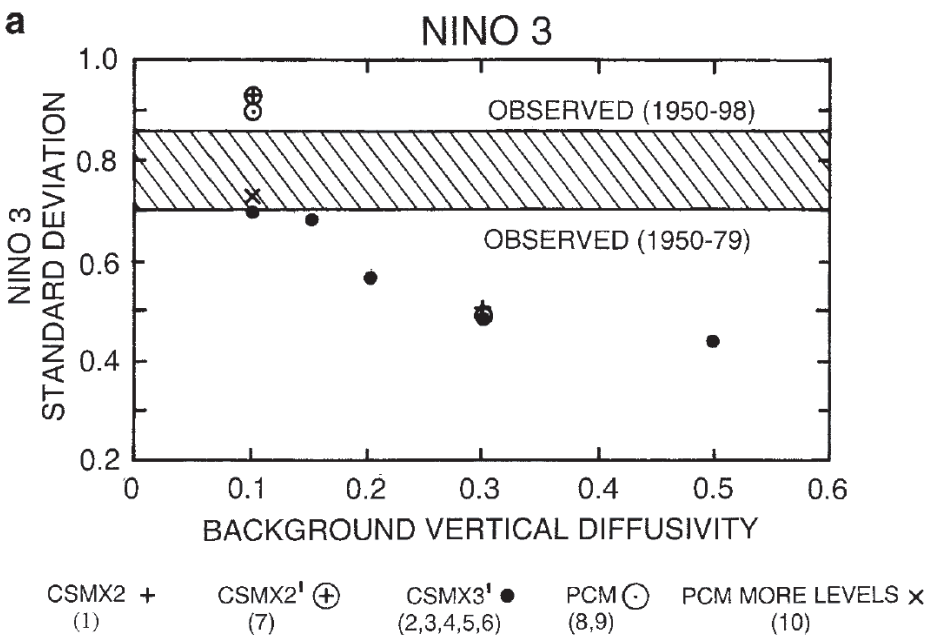

Figure 2: Niño3 amplitude vs. ocean model diffusivity. Nino3 amplitude is the standard deviation of SST (°C) in the Nino3 region (5°S–5°N, 150°W–120°W) for 200-year runs of versions of the NCAR coupled model. Symbols show this amplitude as a function of the background diffusivity (cm^{-2} s^{-1}) used in each model; the monotonic increase in amplitude with decreasing diffusivity illustrates the strong role of cold tongue thermocline-to-surface communication in ENSO. The solid lines show the Nino3 amplitude for available observations for two periods. (After Meehl *et al.*, 2001.)

The unique character of equatorial mixing, which is enhanced due to the high shear above the EUC, depends in turn on the meridional structure of the large-scale currents. Therefore, the vertical-meridional circulation across the cold tongue must be observed and modeled as a whole, and this effort must span scales from the microstructure to the wind-driven divergence and the tropical instability waves. Reconciling the pictures from the different scales is the key to knowing that the diagnoses at each scale are correct. A novel experiment would place turbulence observations in meso- and large-scale context, including the three-dimensional circulation, allowing diagnosis of the complete set of processes for a limited period of time, and thereby sparking the development of model parameterizations for vertical exchange that take into account all relevant factors and scales. PUMP intends to describe the transition of the surface boundary layer from the Ekman-geostrophic regime found poleward of ±5° latitude to the divergent equatorial regime sufficiently well to serve as a challenge to models.

Since we cannot monitor upwelling or turbulent vertical exchanges continuously in the way that Argo, TAO, and altimetry let us monitor gyre circulations, the ultimate goal of this process study is to provide the observations and interpretation that will let basin-scale models accurately represent

these processes based on sparse initialization data. There are four elements to perfecting ocean models for tropical climate forecasting: first, to improve the forcing fields, which requires understanding the effects of short time- and space-scale winds; second, to provide data sets to compare model circulations across the upwelling cell; third, to improve mixing parameterizations through more precise diagnosis of the variability at and near the equator; and fourth, to learn how to use sparse sustained observations assimilated into models to infer and diagnose equatorial mixing and its effects, based on the ongoing ENSO observing system. PUMP addresses all four of these elements.

2. Scientific Background

Our process schematic (Fig. 3) suggests the complexity and interplay of the processes targeted by PUMP. The balance that maintains the equatorial thermal structure (isotherms in black) is that upwelling (large blue arrow) from the equatorial undercurrent (blue arrowhead), driven by near-surface divergence (horizontal blue arrows, due to the prevailing easterly winds [green arrow tails]) is balanced by heating from above (downward red arrows) and turbulent mixing (circular overturns, and also the wiggles on the shallow isotherm indicating internal gravity waves). It is now impossible to be quantitative about any of these processes except in integrals over very large areas and at low frequency. Correctly modeling equatorial circulation and SST variability requires the ability to accurately represent all of these.

A brief review of the present state of our understanding of these processes follows, with an emphasis on some of the most troubling gaps in our understanding. A summary of the gaps that are pertinent to the maintenance of equatorial SST is then presented as a set of focal points for PUMP.

2.1 Upwelling

Upwelling has been identified as a fundamental element of the circulation of the equatorial Pacific (and Atlantic) since the pioneering investigations of

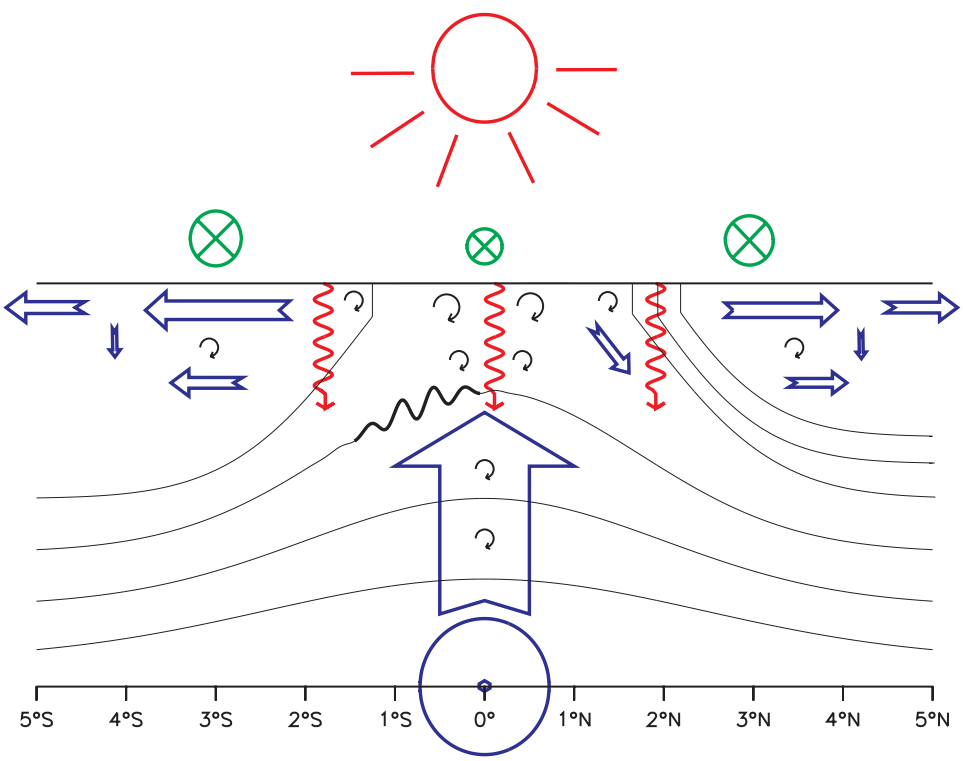

Figure 3: Schematic processes targeted by PUMP. See text for description.

Cromwell (1953), Knauss (1963), and Wyrtki (1981). These studies, and others more recent, have shown that upwelling transport into the upper layer of the east-central Pacific balances the Ekman divergence across $\pm 5°$ latitude, about 30–50 Sv. Part of this transport flows eastward along upward-sloping isopycnals, but there is a significant diapycnal conversion, in which thermocline water flowing into the region at temperatures of 18°–24°C is warmed to flow out meridionally at temperatures 5°C or so higher, a heat gain on the order of 50–80 W m^{-2} (Bryden and Brady, 1985; Weisberg and Qiao, 2000). This entrainment occurs as the surface gains heat through solar shortwave radiation which is spread downwards into the upper thermocline by turbulent mixing. The processes by which this diapycnal conversion occurs and is modulated are key to the variability of the Pacific cold tongue and are a principal focus of PUMP.

From a climate perspective, it is upwelling's role in determining SST that is important. Upwelling is both a response to local winds and a component of the gyre-scale circulation. Each aspect affects SST. In general, the local wind determines the rate of mixing, and how deeply it extends into the thermocline, while the gyre-scale circulation determines the background stratification and the properties of the water that is upwelled (Lu *et al.*, 1998). These properties are a boundary condition for the SST budget.

Several attempts have been made to estimate vertical velocity profiles at the equator from continuity, based on divergence of moored or shipboard horizontal current measurements (Halpern and Freitag, 1987; Brady and Bryden, 1987; Johnson and Luther, 1994; Weisberg and Qiao, 2000; Johnson *et al.*, 2001). Moorings have provided for excellent temporal sampling but have generally been used only right at the equator, while shipboard ADCP samples have shown the complexity of the meridional structure. A caveat for both of these is that errors accumulate in the downward integration, in practice making conclusions about w in the EUC core and below only tentative. It is important to note that because of the difficulty of sampling in the very-near-surface layer (due to aliasing or sound reflections by surface waves), velocities shallower than 20 m are almost never measured, and these divergence estimates have been obtained using some method of extrapolation to the surface. Since this near-surface layer probably contains most of the diverging transport (e.g., Fig. 4), a significant uncertainty remains. Drogued surface drifters have also been used to estimate the horizontal divergence, producing well-resolved depictions of the near-surface flow, but no information about the vertical structure (Hansen and Paul, 1987; Poulain, 1993; Johnson, 2001). Vertical transport averaged over a region can also be estimated (in the mean or low frequency) by indirect methods, based on divergence of geostrophic and (assumed) Ekman transports. The simplest type of estimate is a box surrounding the equatorial region. Geostrophic and Ekman transport across the poleward edges is estimated from zonal isotherm slopes and zonal winds, and some assumptions or estimates made of the zonal flows at the east and west edges (Wyrtki, 1981; Bryden and Brady, 1985; Meinen *et al.*, 2001).

All these diagnoses have come up with similar values for the upwelling required to satisfy the horizontal divergence into the surface layer: a velocity

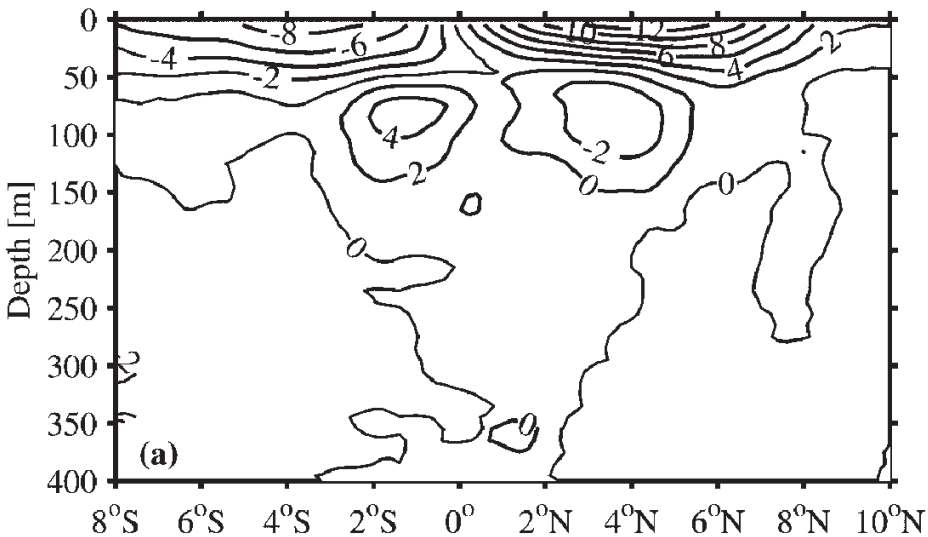

Figure 4: Section of meridional velocity (cm s^{-1}) averaged over 170°W–95°W, from 1991–1999, based on shipboard ADCP sections taken mostly during TAO array service cruises. (After Johnson *et al.*, 2001.)

of a few meters day^{-1}, with a net transport over the cold tongue region of about 30 Sv. The vertical profiles have suggested that w decreases to zero in the lower part of the EUC, and that downwelling occurs below the EUC core, but error estimates have usually shown these deeper values to be at best marginally significant. Perhaps most important for PUMP is the finding from all these studies that only a fraction of the total vertical transport can be accounted for by flow along the sloping isotherms of the equatorial Pacific; and that continuity requires a substantial diapycnal conversion (warming) with some tens of Sv entrained into shallower density levels (Fig. 5). Such entrainment requires some combination of heating from above (for example through penetrative radiation, see section 2.3) and turbulent mixing (see section 2.2).

A crucial feature that has remained essentially unsampled by existing observations is the vertical-meridional structure of the upwelling circulation. The moored time series have all been based on a mooring box spanning the equator, while the shipboard measurements have been seriously aliased by tropical instability waves (TIW). As mentioned above, the near-surface layer which contains most of the poleward limb of the circulation is largely above the sampling depth of the ADCP instruments used in these studies. Model representations of this layer (e.g., Fig. 6) are sensitive to their mixing parameterizations. Nor does theory provide adequate guidance as to how the "Ekman depth" should be expected to change as the equator is approached (McPhaden, 1981). Since vertical velocity is determined locally by the horizontal divergence at each point, these ambiguities imply that we have little idea of the meridional structure and scale of the upwelling, which makes it difficult to infer the timescales on which the circulation should spin up and

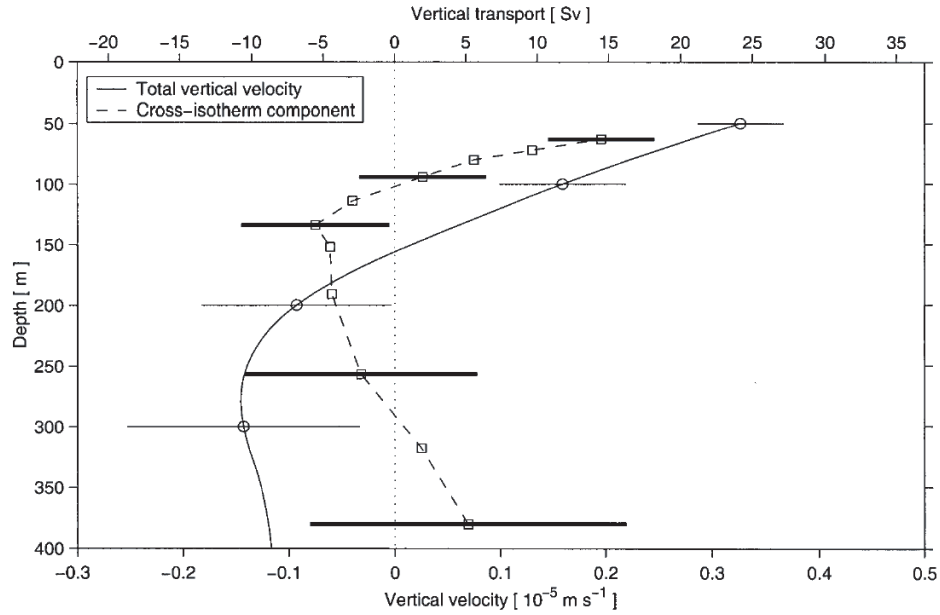

Figure 5: Mean (1993–96) profiles of vertical velocity and transport (integrated over 5°S–5°N, 155°W–95°W). Both the total vertical velocity (w, solid line) and the cross-isothermal velocity inferred by also considering isotherm motion (w_c, dashed line) are shown. The w_c are plotted at the mean depth of isotherms within the region. Isotherms denoted by squares are 10°, 11°, 12°, 13°, 14°, 15°, 17°, 20°, 22°, 23°, and 24°C. Error bars are plotted at representative levels. (After Meinen *et al.*, 2001.)

down in response to wind anomalies. One study based on surface drifters suggested an extremely narrow upwelling scale of about 10 km (Poulain, 1993) which would allow a rapid spinup of small filaments, but in general most researchers have assumed a scale ten times larger and a timescale of weeks or longer.

The meridional structure is complicated by the presence of tropical cells (McCreary and Lu, 1994; Hazeleger *et al.*, 2003; and see Fig. 6) that recirculate a substantial fraction of the equatorially upwelled water above the thermocline, and thereby partly disconnect variations in upwelling transport from the mass exported to the subtropics. Observations and model results suggest downwelling near 3°–4° latitude (Johnson and Luther, 1994; Kessler *et al.*, 1998; Johnson, 2001; Johnson *et al.*, 2001; and Fig. 6), possibly due to the rapid increase in the Coriolis parameter with latitude as the poleward limb evolves toward a true Ekman layer. (But also note that the relative vorticity u_y can be as large as the planetary vorticity f in the strong mean shears between the zonal equatorial currents; u_y augments β roughly between 1°S and 1°N, then reduces β between 1°N and about 5°N.) Subduction of the cool equatorial water beneath the warm water of the North Equatorial Countercurrent is another possibility; this would also contribute to the sharpness of the SST front (section 2.4). Clearly these complex structures depend sensitively on the vertical structure of wind-input momentum

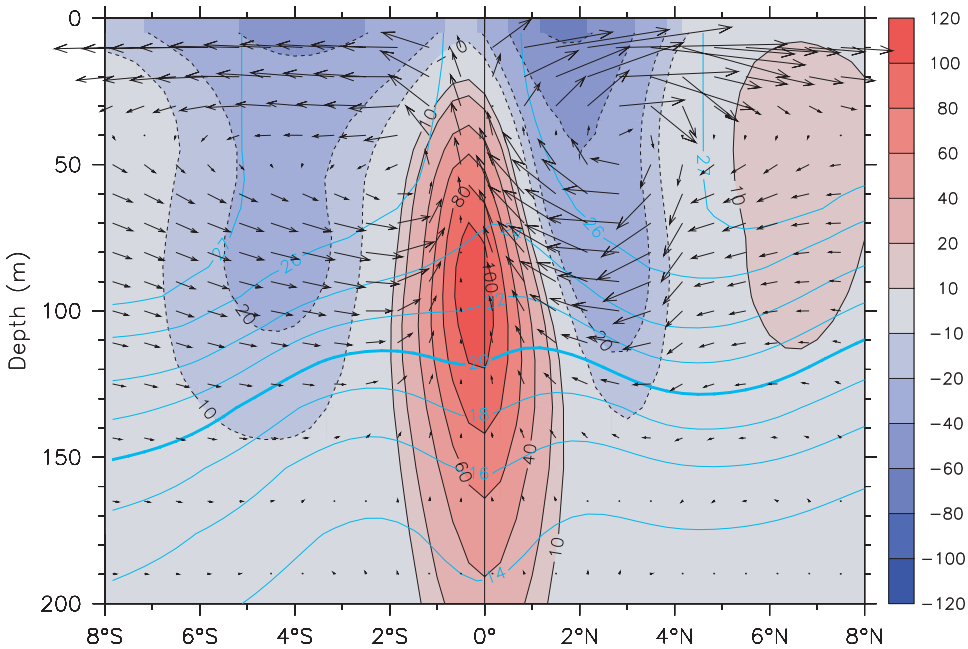

Figure 6: Mean vertical-meridional circulation at 140°W in the MOM2 model. Colors show zonal current in cm s^{-1} (red is eastward, blue westward; scale at right). Vectors show (v, w). Cyan contours show temperature. (Courtesy G. Vecchi.)

and its meridional dependence, especially the poorly sampled near-surface flows.

The PUMP experiment will have to place a major emphasis on resolving the meridional structure of upwelling. This objective is thoroughly intertwined with the mixing observations because the vertical profile of horizontal velocity is determined by how mixing spreads the surface momentum flux downwards.

2.2 Turbulent mixing

The highly sheared current profile above the core of the EUC provided an obvious target for microstructure observations in the early 1970s. These early observations showed low mixing in the EUC core but strong mixing in the high shear zones above the EUC in both Pacific (Gregg, 1976; Crawford, 1982) and Atlantic oceans (Osborn and Bilodeau, 1980; Crawford and Osborn, 1979). From a limited number of profiles they also showed a fairly narrow band of energetic turbulence centered on the equator (Crawford and Osborn, 1981). From these observations, Crawford and Osborn (1979) argued that the turbulent friction in the sheared flow above the EUC core is sufficient to balance the work done by the zonal pressure gradient set up by the easterly wind stress.

The apparent importance of heat and momentum transports by small-scale mixing to the dynamics of the equatorial current system led to three experiments to examine in more detail the nature of turbulent mixing in

the central equatorial Pacific. These were conducted in 1984 (Tropic Heat I), 1987 (Tropic Heat II) and 1991 (Tropical Instability Wave Experiment—TIWE). The sum duration of these intensive profiling observations was about 100 days over a period of 7 years and no intensive profiling has been done since 1991. All of these experiments focused on the site at 0°, 140°W, largely because of the presence of long-term moored observations predating the full implementation of the TAO equatorial array of moorings (McPhaden, 1993; `http://www.pmel.noaa.gov/tao`). These experiments sampled different regimes of the ENSO and seasonal cycles. Tropic Heat I took place in late 1984, during neutral ENSO conditions with a strong EUC and TIW (Gregg *et al.*, 1985; Moum and Caldwell, 1985). Tropic Heat II took place at the end of the 1986–87 El Niño (Peters *et al.*, 1991), and was during the warm season (April 1987), so TIW were weak. The TIWE experiment at 140°W, whose divergence measurements are discussed above, also included a microstructure survey during Nov.–Dec. 1991 (Lien *et al.*, 1995). Other observations have taken place in the quite distinct regime of the west Pacific warm pool during the TOGA-COARE experiment (Smyth *et al.*, 1996).

From these experiments, we gained our first detailed glimpses into the complexity of small-scale processes within the equatorial current system. The intense diurnal cycle of mixing observed in 1984 (Moum and Caldwell, 1985; Gregg *et al.*, 1985) indicated for the first time the departure from steadily forced shear-flow turbulence. The strong latitudinal dependence indicated a departure from the narrow equatorial peak previously observed with more limited observations (Moum *et al.*, 1986; Peters *et al.*, 1988; Hebert *et al.*, 1991). The peak in mixing was observed to extend across the region over which the velocity of the EUC core exceeded 0.25 m s^{-1}, more than 4° of latitude (±2° when the EUC was symmetric about the equator). The decay of turbulence away from the equator was considerably different in 1984 and 1987 across 140°W and different again across 110°W in 1987 (Hebert *et al.*, 1991).

Perhaps more importantly, the diurnal cycle of turbulence was observed to extend into the stratified layers above the EUC core, well below the surface layer that is in direct contact with the atmosphere (Moum *et al.*, 1989). In this depth range the high shear acts to reduce the gradient Richardson number, Ri, to near-critical levels, thereby increasing the potential for shear instability. This deep penetration of mixing was found (in 1987) to be associated with intermittently occurring bursts of high-frequency, internal gravity waves with frequencies near the local buoyancy frequency (McPhaden and Peters, 1992) and wavelengths of 150–250 m (Moum *et al.*, 1992). There are several ways that narrow band internal gravity waves (frequencies near N, 200 m wavelengths) may be generated—candidates include pure shear instability (as indicated by linear stability analysis; Sun *et al.*, 1998; Mack and Hebert, 1997), mixed layer convectively driven eddies (Gregg *et al.*, 1985) and an obstacle effect associated with sheared flow over a perturbed mixed layer base (Wijesekera and Dillon, 1991). While it is possible that different instability mechanisms occur at different times (or even simultaneously), more recent equatorial observations from a neutrally buoyant float clearly show the exponential growth of near-N waves with a 1-hour timescale fol-

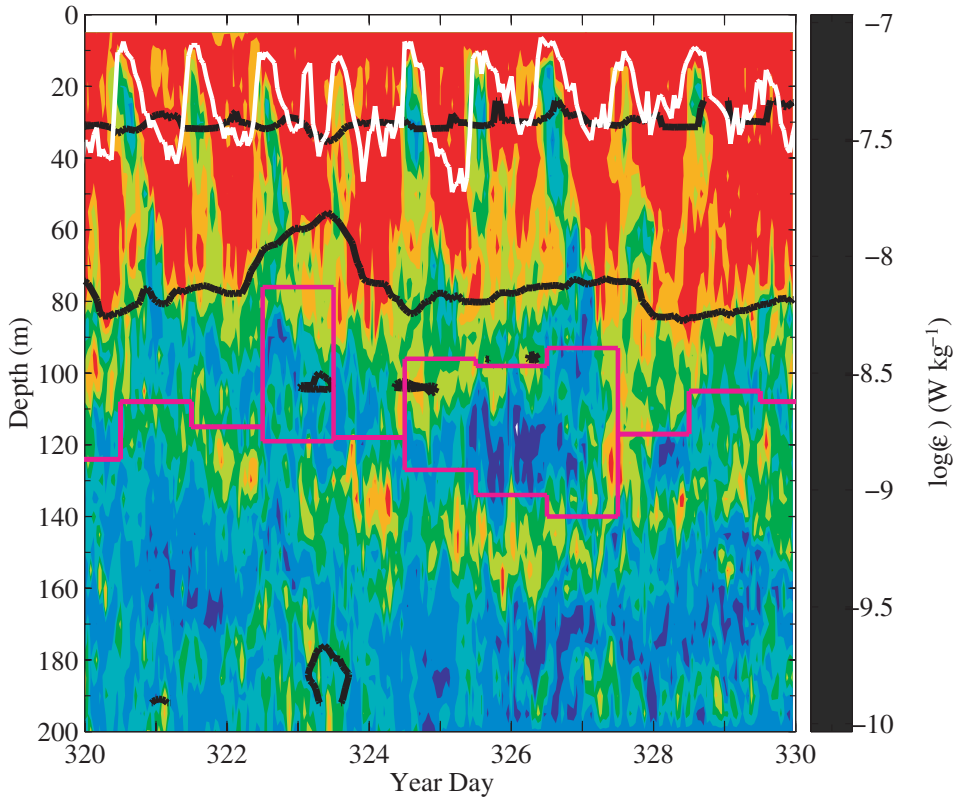

Figure 7: Turbulence dissipation rate ϵ for 10 days of the Tropical Instability Wave Experiment (TIWE) in 1991. The white curve is the mixed layer depth, the black lines delineate where Ri is less than 0.5, and the magenta stairs show the EUC core. (Courtesy R.C. Lien.)

lowed by enhanced mixing (Lien *et al.*, 2002), supporting the idea that shear instability is responsible for internal wave generation and deep-cycle turbulence. An indication of the complexity of mixing at the equator is provided by a 10-day sequence from TIWE (Fig. 7).

The next step in defining the sequence of processes that link the mesoscale to the mixing is to determine the trigger that sets off shear instabilities on a daily time cycle. Our observations of Ri are not sufficiently well-resolved (either vertically, horizontally, or in time) to determine when and where Ri reduces to its critical value. It is not always critical or it would always be mixing, and a consequence of mixing is to increase Ri above critical. It is crucial for us to determine how Ri is modulated in order to make the link to the next larger scale, which is the way we will improve mixing parameterizations.

Modulation of the intensities of both the internal wave field and the turbulence on longer timescales (linked to tropical instability waves, Kelvin waves, and perhaps to El Niño) was determined from a time series of unprecedented length (38 days) obtained by overlapping sets of shipboard ob-

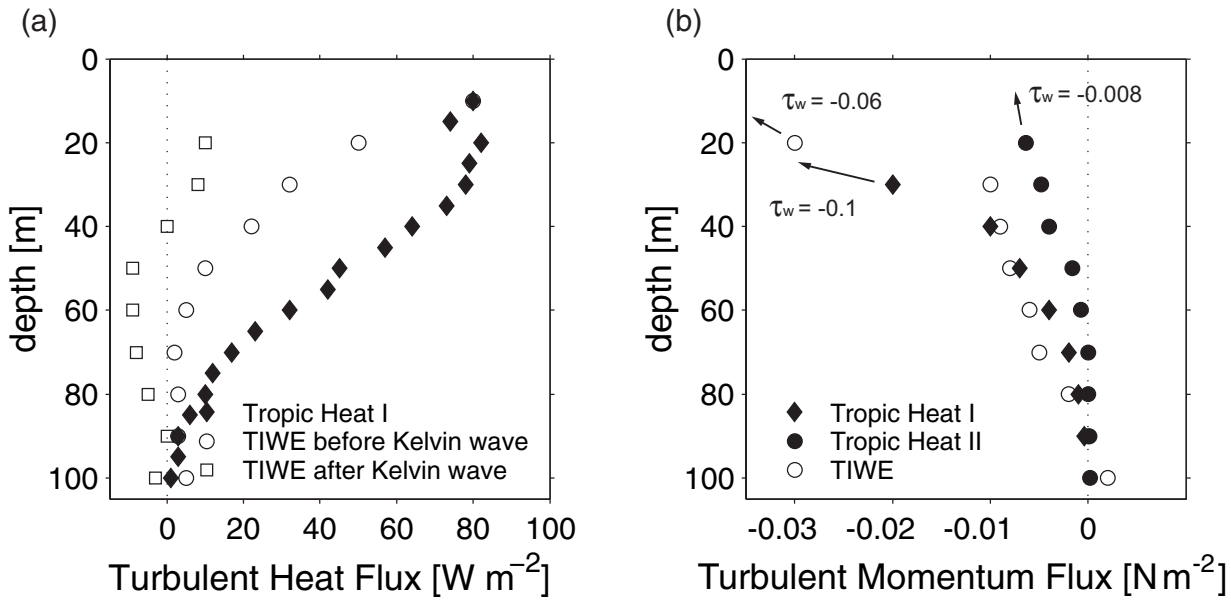

Figure 8: (a) Turbulent heat flux profiles at 0°, 140°W, and (b) turbulent momentum flux (zonal component) profiles from three experiments at 0°, 140°W. In (b), the surface wind stress is indicated by the arrows.

servations by two groups at the same site during TIWE (Lien *et al.*, 1995; Moum *et al.*, 1995).

The role of the turbulence stress divergence (TSD) was examined by Dillon *et al.* (1989) and Hebert *et al.* (1991) from the Tropic Heat 1 and 2 experiments (TH1, TH2). During lower-than-normal winds (TH2) it was found that the TSD played only a small role in the local momentum budget. However, during higher-than-normal winds (TH1), the large near-surface (vertical) transport of momentum (in which the stress profile is approximately exponential and asymptotes to the wind stress at the surface) must be balanced by some other mechanism at intermediate depths, but above the EUC core. Having established the link between turbulence in the stratified layers above the EUC core and internal gravity waves there (however they are generated), it was posited that the apparent momentum imbalance could be satisfied by the vertical transport of momentum by internal waves. This was followed up by theoretical studies that showed how momentum transported by the waves from above the EUC core may act to accelerate currents below the EUC core (Sutherland, 1996; Smyth and Moum, 2002). This has yet to be established observationally. A comparison of turbulent momentum flux profiles from 0°, 140°W (Fig. 8b) shows the variations that have been observed. The differences in the vertical divergences determined from these profiles have yet to be accounted for.

The tenfold day/night difference in heat fluxes was demonstrated by Gregg *et al.* (1985): at 25 m depth, the heat flux increased from 30 W m^{-2} at noon to 240 W m^{-2} at midnight. Over a 12-day period Moum *et al.* (1989) demonstrated that the turbulent flux through 35 m closely balanced

the incoming surface heat flux, including penetrating radiation. The large flux divergence below this must be balanced by lateral or vertical advection. The heat balance varies on a host of timescales, including daily (Fig. 7) and interannual (Fig. 8a). It is difficult to imagine that the large daily changes in turbulent heat flux are matched by changes in upwelling, which must be set by adjustment on larger spatial scale and longer timescale. It is possible that a large scale adjustment mismatch contributes to changing SST on El Niño timescales. Coincident with the passage of a downwelling Kelvin wave observed prior to the 1991–93 El Niño, reduced mixing observed by Lien *et al.* (1995) may have provided positive feedback toward increasing SST in the central Pacific. At the other extreme, enhanced subsurface mixing is a prime (but unproven) candidate for the 8°C surface cooling (in 1 month) at 0°, 125°W to abruptly conclude the strong 1997–98 El Niño (McPhaden, 1999; Wang and McPhaden, 2001). Lagrangian float measurements taken during 1998 showed evidence of enhanced turbulent heat flux in the deep-cycle layer that could help explain the abnormally cold SST during the onset of La Niña (Lien *et al.*, 2002). The inferred intense mixing must also be extremely intermittent and not amenable to observation from infrequent shipboard campaigns of necessarily short duration that must be planned years in advance. This intermittency on long timescales points out the need for not only extended observations of mixing but also a better physical understanding of the generation and evolution of mixing at the equator so that better parameterization can be achieved.

Because of the complexity and strong time-dependence of the mixing above the EUC core (not only on daily, TIW, and Kelvin wave times scales but between independent experiments: e.g., Fig. 8) it has proven difficult to draw unambiguous conclusions from the small number of regimes sampled. Attempts at parameterization are difficult (Peters *et al.*, 1988; 1991), largely because they are based on local observations (local in both time and space). This was clearly acknowledged by Peters et al. and these parameterizations have proven to have only limited utility.

A serious shortcoming of the comprehensive time series measurements to date is that they have taken place right at the equator. We have much less information about the variability of either the shear regime or the mixing just off the equator.

Although we have the tools to measure microstructure from ships for the duration of a research cruise, the wide diversity of turbulence regimes to be studied in the equatorial region poses a challenge that we have yet to meet. It is unlikely that we will be able to measure mixing everywhere it is important. The challenges are

1. to extend mixing observations at one (or a few) locations so that we can resolve the long timescale modulations of mixing that may contribute to El Niño scale events, and

2. develop a better first order understanding of the hierarchy of physical processes that lead to mixing of both heat and momentum so that useful parameterizations of diapycnal fluxes in the equatorial upwelling region can be developed.

We expect this will require a combination of sampling internal wave properties within a detailed observational context, and the use of internal wave models tuned by these observations.

2.3 Heat fluxes

Construction of an empirical heat budget will not only provide insight into the physics of the equatorial cold tongue system, but will also test the consistency of PUMP's measurements and estimates of upwelling and turbulent mixing. During COARE, microstructure measurements, vertical velocity estimates, and surface flux measurements were combined within empirical heat and salt budgets, which closed within the instrumental error bars (Feng *et al.*, 1998; 2000). Budget closure acted as strong evidence that measurements did in fact fall within the expected error estimates.

Since flux fields produced by present-generation atmospheric models can have large errors at specific locations, PUMP will rely on surface flux measurements from its in situ shipboard and mooring platforms. The flux measurements made during PUMP will provide, first, forcing time series for empirical budget analyses, and second, benchmarks for creating flux fields to drive ocean models and to validate air-sea interactions in coupled models. Because a 15 W m^{-2} error in the net surface heat flux applied to a 30 m thick mixed layer can lead to a $\sim$1°C SST error in 3 months (assuming 1-dimensional physics), it is critical that the fluxes be of extremely high quality.

Surface fluxes are the boundary value for the mixing profiles. Therefore, it is standard practice to measure surface fluxes on board ships making microstructure measurements, as was done during the COARE Godfrey *et al.* (1998) and EPIC2001 (Raymond *et al.*, 2004) experiments in the western and eastern tropical Pacific. By similar arguments, surface flux measurements should be colocated with vertical velocity calculations so that full 3-dimensional heat and momentum budgets can be evaluated at these locations.

Solar and longwave radiation can be measured from radiometers mounted on ships (Burns *et al.*, 2000; Fairall *et al.*, 2003) or buoys (Weller and Anderson, 1996; Cronin and McPhaden, 1997; Cronin *et al.*, 2004). Latent and sensible heat fluxes can be measured directly from a covariance method (Reynolds stress) from ships or from buoys using bulk algorithms. The bulk (latent and sensible) heat flux algorithm developed for the western equatorial Pacific warm pool during COARE (Fairall *et al.*, 1996) and later modified for other regions (Fairall *et al.*, 2003) has an accuracy of 5–10 W m^{-2} in scatter from direct measurements. Errors in the algorithm input measurements (relative wind speed, air temperature, SST, specific humidity) propagate through the algorithm and lead to additional errors, typically less than 10 W m^{-2}.

OGCMs have demanding requirements for high-quality forcing. Gridded solar and longwave radiation can be obtained from satellites, in combination with radiative transfer models and other data as is done by the International Satellite Cloud Climatology Project (ISSCP) (Rossow and Zhang, 1995). Er-

rors in these radiative fluxes are up to 20 W m^{-2}. However, latent and sensible flux fields generated by atmospheric numerical prediction models (e.g., NCEP) can have large errors when compared to moored flux measurements. In a comparison of the seasonal cycle from 7 years of data (1991–1997) at four sites along the equator including 140°W, Wang and McPhaden (2001) showed that the available flux products differed among themselves in both magnitude and phase, with a range of discrepencies as large as 60 W m^{-2}. Not surprisingly, OGCMs forced with numerical weather prediction (NWP) flux fields rapidly drift from reality. For this reason, OGCMs typically treat surface fluxes as a mechanism to relax model surface fields back to a known field (e.g., climatology or a reanalysis product) and may have no direct relation to physical meteorological events. A new tack in creating gridded flux fields is to use a blend of satellite fields with NWP output in combination with a state of the art bulk algorithm (Yu *et al.*, 2004). PUMP modeling efforts are likely to rely upon these types of new flux fields, tested and verified against PUMP flux measurements.

Recent modeling studies (Nakamoto *et al.*, 2001; Murtugudde *et al.*, 2002) have focused attention on the fact that the high biological productivity of the equatorial cold tongue can have significant effects on the vertical profile of solar heating. Models have traditionally assumed the heating due to attenuation of solar radiation by phytoplankton and water to be well represented by a constant attenuation term, typically $\sim$0.04 m^{-1}. For the equatorial Pacific upwelling region, and much of the global ocean, this is an underestimate. In fact the growth of phytoplankton often results in the absorption of shortwave radiation within the mixed layer, where the usual model allows some of that to penetrate through. The complexity of biophysical modeling studies in the equatorial Pacific is increasing—recent work incorporates a hybrid coupled atmosphere-ocean-ecosystem model.

If PUMP is to aim for closure of the upper ocean heat budget to within $\sim$10 W m^{-2}, then the radiative heat flux must account for both the temporal and spatial (both horizontal and vertical) variability of chlorophyll. Mixed layer heating rates due to typical chlorophyll concentrations can vary by 10 W m^{-2}. For the PUMP intensive observing periods (IOPs), quantifying radiant heating to the required accuracy will be possible using profiling radiometers deployed from ships, radiometers attached to floats or gliders, or by accurately mapping the spatial and temporal chlorophyll variability from CTD profiles. Outside of the IOPs, moored radiometers could provide attenuation profiles, or satellite chlorophyll measurements could be used to estimate mixed layer radiant heating (Ohlmann, 2003; Strutton and Chavez, 2004).

2.4 Frontal processes

An important feature of the equatorial ocean is the front (depicted near 2°N in Fig. 3) separating the cold tongue from warmer water along the North Equatorial Countercurrent (NECC). The front is poorly resolved by in situ monitoring observations, and is subgridscale in existing climate models. Thus, the front is a relevant target in any process study whose ultimate

goal is to improve parameterizations. Fronts may exist for a variety of reasons, but in the open ocean fronts are inevitably caused by convergence in the across-front direction (often visible as linear slicks; Yoder *et al.*, 1994). This convergence may be balanced by vertical divergence, so fronts are often accompanied by a vertical circulation. Fronts are regions of enhanced vertical shear (Fig. 9), especially if they are geostrophically balanced near the equator, possibly leading to enhanced mixing. In mid-latitudes, fronts are known to have associated across-front ageostrophic circulations, responsible for downwelling/upwelling on the dense/light side of fronts. Such a circulation, diagnosed using the omega equation (Rudnick, 1996), may also exist at the equatorial front, and may explain the spatial structure in vertical flows. Finally, the equatorial front must be monitored to provide context for the vertical microstructure profiles, as oceanographic conditions change so strongly across the front.

The tropical instability waves that produce the prominent meridional motion of the front are easily observed in satellite SST (Legeckis, 1977), with timescales of order 20 days and length scales of several hundred kilometers (Fig. 10). TIW are also observed in satellite altimetry (Weidman *et al.*, 1999), surface drifter tracks (Hansen and Paul, 1987; Flament *et al.*, 1996; Baturin and Niiler, 1997) and moored temperature and velocity time series (Halpern *et al.*, 1988; McPhaden, 1996), and are a robust and commonly observed aspect of the eastern tropical Pacific (and Atlantic). As such, TIW influence all aspects of the observational program proposed here. In addition they are a ubiquitous feature of ocean GCMs (Cox, 1980; Masina and Philander, 1999; among many others). With very large velocity fluctuations, on the order of ± 50 cm s^{-1} at the equator, TIW are a substantial source of noise in typically sparse ocean observations that pose difficult aliasing problems, even to sample the mean (Johnson *et al.*, 2001). However, moored velocity time series off the equator are lacking, so much of the interpretation of the TIW velocity field has been based on surface drifters, while the off-equatorial subsurface flows and shears remain unknown. TIW propagate west with speeds of 30 to 60 cm s^{-1}, weakening west of about 150°W. A fact that has caused confusion is the difference in apparent frequency depending on the quantity being observed, with SST showing a dominant period of about 25 days (Legeckis, 1977) whereas thermocline depth has a period near 33 days, and equatorial velocity a period near 17 days (Lyman *et al.*, 2004). Although the TIW were first identified north of the equator, and their strongest signals are found there, recent work has shown evidence of TIW signatures in the south (as suggested in Fig. 10).

The principal mechanism producing TIW is thought to be barotropic (shear) instability as first explained by Philander (1976; 1978), but there has been an evolution in thinking about this problem. Since it is very difficult to diagnose energetics from sparse ocean observations, most of the work has been done in numerical models (but see Luther and Johnson, 1990, and Qiao and Weisberg, 1998, for observational diagnoses). The original Philander analysis concluded that the relevant shear was near 4°N between the eastward NECC and the westward South Equatorial Current (SEC). More recent work points to the shear closer to the equator between the SEC

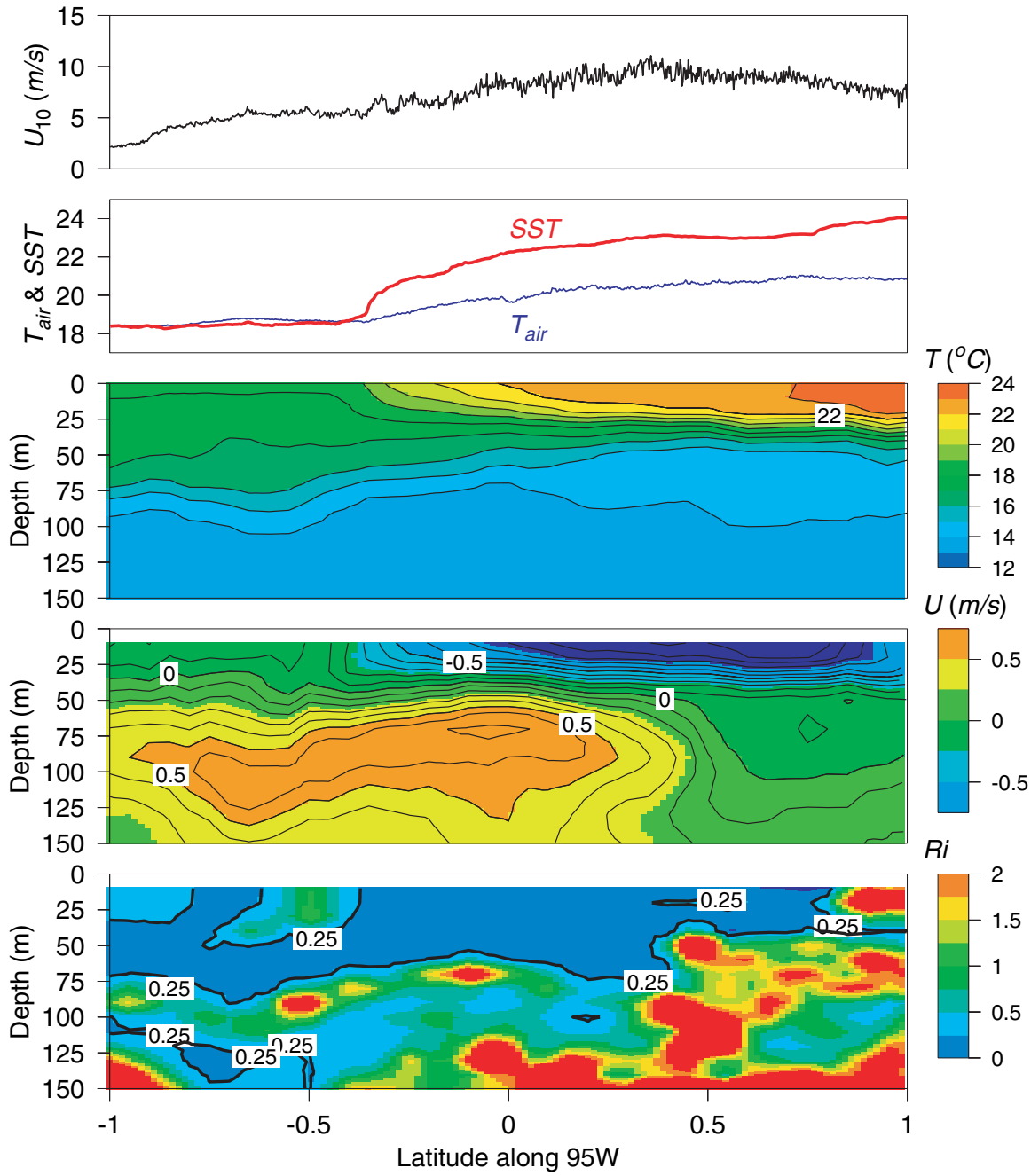

Figure 9: Atmospheric and oceanic conditions across a sharp front in a detailed meridional section along 95°W during EPIC 2001. From the top, plotted are wind speed, sea surface temperature, air temperature, and sections of temperature, eastward velocity, and Richardson number (Ri) calculated on a 10 m vertical scale. In the atmosphere, high frequency wind variability changes markedly across the front, suggesting a strong gradient in air-sea fluxes. In the ocean, large velocity shear leads to low Ri in a region of strong stratification and presumably vertical mixing. (Courtesy Wijesekera, Paulson, and Rudnick.)

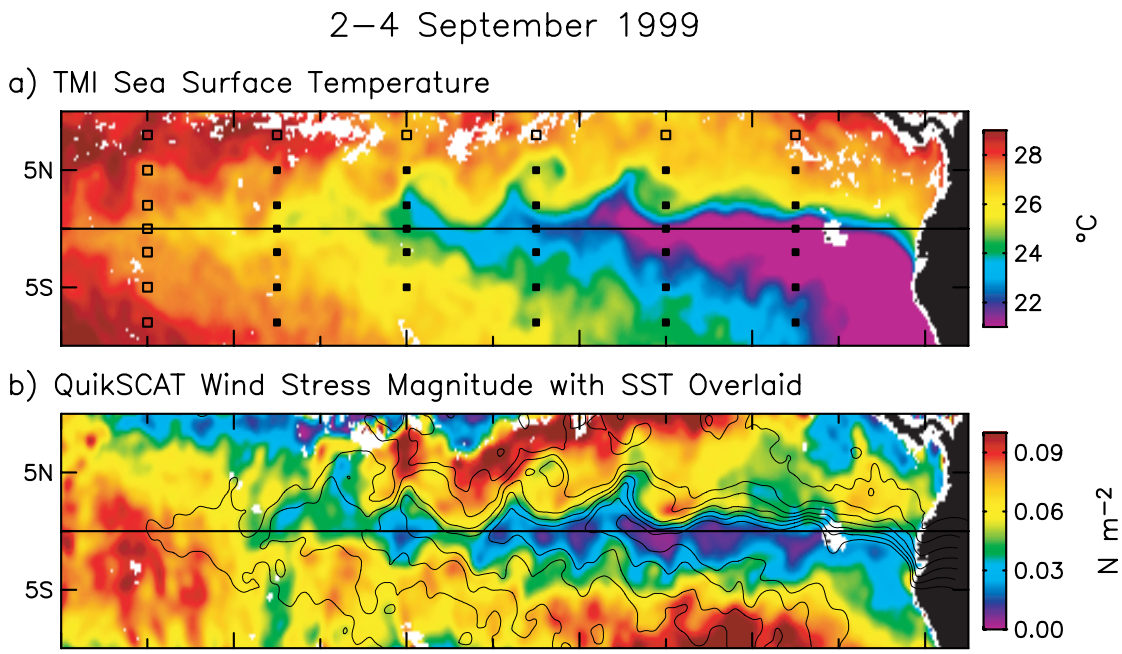

Figure 10: Example of the sensitivity of winds to SST. Top: SST measured by the TRMM microwave instrument during 3 days in September 1999. Note the sharp front north of the equator that is distorted by tropical instability wave cusps. Bottom: Quikscat wind stress magnitude (color), with overlaid SST contours. Note the close correlation of windspeed with SST in the frontal region. Since the winds in this region are southeasterly, the rapid speed change as the winds blow across the SST front indicates the short timescale of boundary layer response to SST. (After Chelton *et al.*, 2001.)

and the EUC; in addition the possibility of baroclinic instabilities associated with either the spreading isotherms around the EUC or with the temperature front may be important as well (Yu *et al.*, 1995; Masina *et al.*, 1999). The sources of energy conversion driving the TIW remains an active area of research, and it is likely that different mechanisms come into play at different latitudes, perhaps explaining the multiple frequency structure seen (Lyman *et al.*, 2004). However, the fact that OGCMs of diverse types readily generate TIW, whether forced with realistic or highly simplified winds, suggests that near-equatorial shear is the dominant factor.

Because TIW depend on background conditions, which vary seasonally and interannually, their low-frequency modulation is expected. The entire upper equatorial circulation quickens when the winds are strongest in June–December: the SEC and NECC are largest in boreal fall, as is upwelling. These conditions produce both the strongest shears and temperature front, so it is not surprising to find that the TIW begin to appear in June–July, grow stronger through the second half of the year, and persist until February–March. Similarly, during El Niño events both the SEC and the cold tongue weaken, and TIW are absent (Baturin and Niiler, 1997).

Observational diagnoses conclude that tropical instability waves contribute to the heating of the cold tongue at a similar magnitude as solar

radiation (Hansen and Paul, 1987; Bryden and Brady, 1989; Baturin and Niiler, 1997; Swenson and Hansen, 1999). OGCMs have provided useful hints to the heat balances of TIW (Masina *et al.*, 1999), but suggest that the observational estimates may be overestimated due to inability to measure vertical TIW fluxes (Jochum *et al.*, 2004).

The instabilities may intensify enough to form vortices (Flament *et al.*, 1996). In this manner, fluid from one side of the front may become trapped on the other, just as warm core rings are trapped inshore of the Gulf Stream. The net effect of meridional movement of the front is probably not reversible. By advecting warmer off-equatorial water above the colder upwelled equatorial water (Fig. 9) vertical gradients become enhanced, increasing the heat flux due to vertical mixing.

Other processes influencing the formation and maintenance of the front include meridional gradients in the vertical velocity field and surface forcing across the front. EPIC results have shown that surface fluxes tend to warm surface water in the cold tongue region and cool waters to the north. Thus meridional gradients in surface fluxes tend to damp the front.

The existence of the sharp front contradicts the picture of Ekman divergence moving substantial quantities of equatorially upwelled water directly into the northern hemisphere subtropics. Some of this water must be downwelled at the front. Off-equatorial downwelling has been observed and modeled in this region, which has been attributed to large-scale dynamics (section 2.1), but it is likely that this is only part of the answer. Across-front transport through along-front instabilities may prove to be important, and could be a key process missing in climate models.

The sharpness of the front (Fig. 9) suggests that significant improvements in our ability to describe and model the upwelling regime will require much denser sampling than previous 100-km scale buoy programs have provided. On the other hand, variability during the roughly one month that a ship can remain on station is dominated by the phase changes of the TIW and the position of the ship relative to the moving front. Therefore, a description of the fluctuations of the front in the presence of TIW requires both moored time series to establish the regional gradients and to resolve the short timescales, as well as shipboard sampling that can follow the front and adequately sample its small spatial scales.

2.5 Ocean-atmosphere feedbacks

Because equatorial zonal winds are sensitive to SST gradients on short time and space scales, upwelling events have the potential to interact rapidly with the wind and thus produce coupled feedbacks. These scales are on the order of 1 day and a few tens of km, illustrated by the large windspeed changes as southeasterly trades blow across the SST front north of the cold tongue (Fig. 10; Chelton *et al.*, 2001). The sensitivity arises because cool SST stabilizes the atmospheric planetary boundary layer and thus disconnects it from the stronger winds aloft (Chelton *et al.*, 2001). Over warm SST, by contrast, convection efficiently mixes momentum, which generally speeds up the surface wind. Both the intensification of winds and the small scale

variability associated with boundary layer turbulence are evident on the warm side of the front shown in Fig. 9. Thus an upwelling (cooling) event can potentially feed back to weaken the wind that drove it, on a short timescale. It remains to be seen how effective this mechanism is at modulating the upwelling circulation. Most observations of this phenomenon have focused on the region east of about 125°W, because the SST front is strongest there and the effect is most visible; it is not known whether small SST gradients will produce significant feedbacks.

On the scale of hundreds of kilometers, the interaction of the zonal SST gradient and zonal winds is the basis for "SST modes" (Neelin *et al.*, 1998), in which SST anomalies are produced by $w\partial T/\partial z$ due either to anomalous upwelling itself or to anomalous thermocline depth that changes the temperature of the upwelled water. Coupled modes arise because SST gradients then produce wind anomalies which further modify w. Such modes can propagate either eastward or westward, depending on the relative importance of these two processes, and probably contribute to the evolution of El Niño events.

Another form of feedback can occur because cool SST is favorable to the formation of the stratocumulus decks that cover much of the eastern tropical Pacific, especially in the south. Although this positive feedback is clearly of major importance to the surface-layer heat budget, it is not known what factors balance it, nor is it known how the stratus response varies depending on the initial SST.

2.6 Gaps in our understanding of the processes that modulate equatorial SST

1. What is the meridional scale of the upwelling?

   Is it broad and slow, or thin and filamentary? How does it spin up or down in response to changes in the zonal wind? How does the spinup vary with latitude? How deep does it reach into the stratified layer? The structure of the diverging surface layer is almost completely unknown, but the details of the hard-to-measure near-surface velocities determine the width and thickness of the upwelling (section 2.1). With even the best models using a typically 10 m vertical grid spacing, it is hard to have confidence in their simulations of these small scales. In addition to upwelling at the equator, observations and models suggest downwelling at roughly ±3–4° latitude. Is this associated with the SST front north of the cold tongue? What processes strengthen and weaken the front?

2. What is the spatial structure of equatorial mixing?

   Is it closely trapped to the equator (where almost all measurements have been made) or does it occur more regionally? Does the latitudinal variation of background shear determine the structure of mixing? Is the mixing sporadic in space and time, or can it be characterized by larger scales?

3. What causes modulation of the turbulence in stratified layers above the EUC core?

   While it is clear that mixing varies by orders of magnitude over the course of the ENSO and annual cycles (section 2.2), we do not yet know what factors instigate the instabilities leading to enhanced deep-cycle mixing on a daily cycle. We thus cannot infer what mixing will be under any particular circumstance.

4. What are the surface heat fluxes?

   Heat flux estimates quantify the exchange of heat between the atmosphere and ocean, but have a large and poorly known uncertainty. Errors in surface forcing are one of the largest contributors to errors in ocean model simulations. Within the ocean, the transmission profile of solar radiation through the water column is just beginning to be explored, and appears to be highly variable. In particular, the role of biology in controlling the penetration depth appears to be complex and allows the possibility of feedbacks (section 2.3).

5. What is the role of the SST front in modulating equatorial SST?

   What is the magnitude and mechanism of heat fluxes induced by the propagation and instability of the SST front which has a mean location north of the equator but which is advected to and even across the equator by TIW? Mixing across the front is potentially large, both on the 1–10 km frontal scale and on the 100 km TIW scale, but the mechanisms that produce this mixing remain obscure (section 2.4).

6. What are the ocean-atmosphere feedbacks due to upwelling?

   Satellite scatterometer wind fields have shown that SST variations feed back on the atmospheric planetary boundary layer, producing distinct wind regimes as a function of SST (note the smaller green wind vectors over the cooler equatorial water in Fig. 3). Forecast models must account for these interactions, which couple SST and the PBL. Since the wind variations also modify the latent heat fluxes, this coupling involves all the forcing terms of the region (section 2.5).

3. Implementation of PUMP

3.1 Objectives of the PUMP field program

Objective 1: To observe and understand the evolution of the near-equatorial meridional circulation under varying winds, sufficiently well to serve (a) as background for the mixing observations in objective 2; (b) as a challenge to model representations. The observations must be conducted on a spatial scale to usefully compare to and verify modern OGCMs, and be sampled sufficiently often to determine the timescale of adjustment to changes in surface wind stress.

Objective 2: To observe and understand the mixing mechanisms that determine (a) the depth of penetration of wind-input momentum as a function of latitude, time and background conditions; (b) the penetration of surface heat fluxes into the upper thermocline and the maintenance of the thermal structure in the presence of meters/day upwelling. Further, to describe the environmental context of these mechanisms so as to enable the development of model parameterizations.

Objective 3: To construct a surface heat budget of sufficient accuracy to serve as a useful boundary condition for objective 2. This will include a reconciliation of advective, mixing and surface flux influences on the heat and momentum budgets.

Objective 4: To observe and understand the relationship between lateral and vertical processes promoting diapycnal mixing, especially the exchanges across the SST front north of the cold tongue. To decipher the exchange mechanisms, both the scale of the sharp front (1–10 km) and of the TIW (100 km) must be observed.

To achieve these objectives requires a coordination of historical data analysis, modeling, and both long-term and intensive observations. A general plan and justification for each component is proposed in section 3.2.

PUMP will require a substantial in situ observing program with overlapping sampling elements to resolve the necessary spatial and temporal scales. The observations should include both moored time series for their temporal resolution and ability to provide continuous sampling over a 2-year experiment, and shipboard surveys to resolve the smaller-scale features and study detailed mixing processes. PUMP will be embedded within the TAO array, so as to take full advantage of the long TAO time series.

Location of the PUMP field program

PUMP observations should take place along the 140°W TAO mooring line. This location has been the site of many observational programs based on the TAO velocity and temperature time series and on numerous cruises of diverse types (sections 2.1, 2.2, 2.3), and is within the cold tongue regime, although weaker than further east. Most previous tropical Pacific work on both divergence and turbulent mixing, as well as the only local (shipboard)

observations of the TIW front (Flament *et al.*, 1996) have been at 140°W. This long history provides for maximum context to assure representativeness. 140°W is optimal for sampling the processes that govern the Pacific overturning circulation, and results should be applicable to a wide range of longitudes from at least 120°W to the Dateline. This is most important in advancing the ability to diagnose and forecast ENSO variability. The upper layer is sufficiently thick at 140°W so that a reasonable vertical distribution of moored samples (5 m) can assure adequate resolution, as well as giving confidence that model simulations (on a similar scale) can resolve the acting processes.

An argument can be made for siting the PUMP experiment further east, at either 125°W or 110°W, where the cold tongue and SST front are more intense (Fig. 10), and where the results may be more easily integrated with the findings from the EPIC program. A site further east might better address the frontal (section 2.4) and air-sea interaction (section 2.5) elements of PUMP. 110°W has a similar record of TAO velocity and temperature time series, although it lacks a history of microstructure sampling. Three factors militate against doing PUMP at 110°W: First, with mean zonal winds at 110°W only half as strong as at 140°W, it is less clear that this longitude is representative of the upwelling/mixing regime of the central Pacific. Second, the circulation along 110°W is strongly affected by the prevailing meridional winds and is thus highly asymmetric and more complex. Third, the upper layer is so thin at 110°W that resolving the vertical structure so as to disentangle the various influences on the heat and momentum budgets is much more demanding, both in observations and models. While variability at 110°W is unquestionably of great importance, it appears to be a more difficult problem that may become more tractable once the mechanisms in the central Pacific have been more fully elucidated.

The site at 125°W might be an appropriate compromise from the standpoint of physical processes. However, the fact that there is no history of velocity measurements there, in contrast to the 20-year histories at 110°W and 140°W, means that the background to interpret the PUMP observations would be lacking. In addition, previous microstructure sampling has been at 140°W. Since even the two years of PUMP is a short time in the context of the annual cycle and ENSO, we believe it is critical to choose a site where the irreplaceable time history of TAO temperature and velocity measurements exist.

We do advocate a Phase II of PUMP to repeat the 140°W study further east at 110°W, where the SST front is more intense and it is possible that local air-sea interaction is stronger. This should follow analysis and careful consideration of the results from an experiment at 140°W. The challenges of obtaining meaningful observations in the thinner upper layer at 110°W must be a focus for success at this location. However, the focus of PUMP as outlined here should be on the connection of the thermocline to the surface mediated by upwelling and turbulent mixing. That is most likely to succeed in the relatively straightforward environment at 140°W. However, progress in understanding the zonal structure of equatorial turbulence can be made during PUMP by deploying Lagrangian shear-measuring floats that would

extend the sampling over a range of longitudes and help to put the PUMP measurements in a larger-scale context.

3.2 PUMP components

3.2.1 Historical data analysis

Specific Objectives:

- Assess uncertainties on mixing and divergence estimates through an integrated reanalysis of existing data sets.
- Expand the range of climate states for future model parameterization by coordinating a general analysis and making these data generally available.

As part of the larger goal of improving parameterizations of mixing at the equator, it is important that a unified analysis of the data obtained in the Tropic Heat I, II, and TIWE mixing experiments be a part of the final product of PUMP. These data will then become part of the community data set.

One aspect of this component that is important at an early stage of this project is an assessment of the uncertainties of our mixing measurements. In particular, in section 3.2.3 we propose to make intensive measurements of mixing and obtain longer time series of mixing (but with less vertical resolution) at a few moored locations on and north of the equator. Can we thereby obtain a meaningful projection of the integrated turbulent heat flux over the experiment domain for the duration of the experiment? We have considerable confidence in both our method for estimating turbulent dissipation rate (Moum *et al.*, 1995) and in our heat flux estimates from these (Moum *et al.*, 1989; also the NATRE results—Ledwell *et al.*, 1995). The more serious problem in obtaining meaningful averages is the natural space/time variability of the turbulence. The overlapping TIWE microstructure data sets have shown us the consequences of the tremendous geophysical variability over short time and space scales (Moum *et al.*, 1995). Differences in ϵ on hourly timescales from data obtained at the same depth from two ships within 11 km of each other were occasionally several factors of 10. These differences reduced to a factor of 3 on daily averages and were undetectable on 3.5-day averages (the duration of the overlap).

The close agreement on the 3.5-day timescale gives us some confidence that sufficiently long time series can provide meaningful averages over spatial scales that are representative of the same flow regime (O(100 km)?). However, this has not been tested. One way to evaluate this is with a reanalysis of the cross-equatorial turbulence data obtained in Tropic Heat I, II (Hebert *et al.*, 1991) with the specific objective of determining the space/time variability of the turbulent heat flux across the equator.

Other elements of historical data can also contribute to assessments of uncertainty and representativeness of the proposed measurements. The long time series of velocity, temperature, and surface meteorology at the 0°,

140°W TAO mooring is of course a principal reason for siting PUMP at that location, but in addition there are many shipboard ADCP sections taken during mooring service cruises (Johnson *et al.*, 2002), which provide our principal source of information on the meridional structure of velocity. These data are the basis for the preliminary scale analysis shown in Fig. 11, but more could be done, for example by using satellite data to stratify the ADCP sections by the TIW phase. Second, more use could be made of the moored velocities sampled during TIWE, which uniquely included off-equatorial moorings at 1°N and 1°S (Weisberg and Qiao, 2000) and thus contain information on the meridional structure that has barely been looked at. In addition, an opportunity was neglected in the TIWE program by not considering the microstructure data in light of the velocity time series that Weisberg and Qiao (2000) used to estimate divergence. In essence these two data sets were studied in isolation, though being collected at the same time and place. A joint analysis of these time series would have similarities to a less ambitious PUMP experiment, and would aid in designing the PUMP observational strategy.

3.2.2 Time series: Seasonal and interannual variability across the cold tongue

Specific Objectives:

- Determine the structure and the patterns of variability of horizontal velocity in the vertical-meridional plane across the cold tongue at 140°W over at least two annual cycles.
- Determine the spinup of the poleward surface limb of the meridional circulation under varying winds so as to describe and diagnose the evolution of the "Ekman layer" approaching the equator.
- Determine the vertical-meridional structure of horizontal divergence and consequent upwelling velocity across the cold tongue. Describe the corresponding variability of temperature (and ideally salinity).
- Determine the downwelling that occurs at the SST front north of the cold tongue, and its relation to wind forcing and to tropical instability wave variability.
- Ultimately, assess the diapycnal conversions necessary to account for the coincident velocity and temperature variability, in order to diagnose these in light of the heat fluxes associated with turbulent mixing.

To achieve these objectives, the horizontal velocities must be measured at scales sufficient to take meaningful horizontal derivatives. Since PUMP is concerned with the entire meridional circulation, not just the equator, the observations must extend over at least ±3° latitude. The velocity measurements must resolve the vertical structure, and must adequately sample the flow to within a few meters of the surface, where most of the poleward flow

occurs (e.g., Fig. 4). Variations within a tropical instability wave cycle (20–25 days) must be resolved. Because of the very large signals due to these waves (instantaneous v 5–10 times as large as the mean), as well as other high-frequency variability, the sampling must be made at high temporal resolution (hourly), and must extend over a long enough period to define means and variances (2+ years). Concurrent measurements of temperature (and salinity where possible) are needed to construct a heat budget.

These requirements point to moored platforms as the primary observational tool. Modern moorings provide the high sampling rates and long endurance suitable for the temporal demands of PUMP. Coincident velocity and temperature profiles can be obtained (potentially salinity as well), and a combination of ADCP profilers and near-surface point current meters can measure velocity over the entire upper water column from 300 m depth to just below the surface. Moorings also allow for simultaneous water property and surface wind and flux measurements, as well as serving as a platform for other technologies, such as long-term microstructure sampling, that are under development (see section 3.2.b), and sampling of the biology and its effects on heat absorption. The 2-year moored velocity and temperature time series across the equatorial zone will enable a diagnosis of the dynamical transition from the mid-latitude Ekman-geostrophic regime to the equatorial regime.

Other techniques are potentially available to sample the vertical velocity, including floats that may be able to measure w directly (Barth *et al.*, 2004), have been suggested. While such instrumentation may be useful during the short-term IOPs (section 3.2.3), floats are unlikely to remain in the vicinity of 140°W for very long. Thus they cannot serve the purpose of providing the background time series, spanning frequencies from hourly to annual, that will be necessary to interpret the IOP measurements, which will be dominated by the monthly timescale of TIW.

Decades of experience during the TAO project have shown that these moorings serve as fish aggregators, and spurious reflections from the schools can be a serious contamination to the velocities observed by ADCPs. For this reason, subsurface, upward-looking ADCPs are used, which must be separated from the associated temperature/surface meteorology mooring by a few kilometers. The PUMP plan envisions such dual mooring pairs, with the surface moorings supporting the near-surface velocity sampling, as well as the necessary surface flux, temperature, salinity, microstructure, and other instrumentation.

Several questions must be answered in developing a moored sampling strategy for PUMP. Two sources of error are likely to occur, both of which are amplified by taking derivatives. First are errors due to inadequate sampling of the geophysical scales of the velocities. Second are instrumental errors that result from mooring technological limitations. Previous studies calculating divergence from moorings have focused their error analysis on estimates of the mean, in which averaging over a large number of samples reduces some sources of uncertainty (e.g., Weisberg and Qiao, 2000). In PUMP, where we intend to resolve velocity variability on timescales of a week, we will not have this advantage.

Two main sources of instrumental error have been identified by previous studies, and will be unavoidable during this experiment as well: compass errors, which are as much as 2°, and uncertainty of the mooring position due to its watch circle, which is unknown for a subsurface mooring, but could be as large as ±2 km. Compass errors are magnified in the situation where one velocity component (v) is small compared to the other (u), because the measured velocity effectively rotates some of the strong (zonal) current into the weak (meridional) current. Weisberg and Qiao (2000) showed that for the 0°, 140°W site in the worst case (oppositely directed offsets on moorings between which $\partial v/\partial y$ is to be estimated), the compass-produced error in Δv is approximately $u \sin(4°)$. At the equator, this is as large as 7 cm s^{-1}, about 20% of the magnitude of historical moored v, but will be smaller away from the EUC. Watch circle uncertainty produces an error in Δy used for the finite differencing. If $\partial v/\partial y$ is taken over small Δy, then both these errors are magnified in importance relative to the signal measured. Thus, although it might seem to be an advantage to space the moorings closely, in fact it is important to choose a spacing that maximizes the signal, by using a Δy appropriate to the scale of v.

There is little information about the meridional structure of near-equatorial meridional velocity, except in the mean (Johnson *et al.*, 2001; see Fig. 4). That study was based on shipboard ADCP data taken during the roughly twice-yearly cruises made to service the TAO moorings, and showed that only by averaging the infrequent snapshots over the entire data record and over longitudes from 95°W to 170°W could a meaningful mean divergence be constructed, primarily because of TIW aliasing. However, these data can be used cruise by cruise to estimate the meridional scales of nearly-instantaneous v across the cold tongue region (Fig. 11), which is a more stringent test than the weekly averages demanded by PUMP. Eight cruises spanning 1996–2001 were studied, and the decorrelation length-scale of v over 2°S–2°N during the individual cruises ranged from about 0.3° to about 1.2° latitude, with an overall average of about 2/3°. Inspection of v from the cruises suggested that a 2/3° buoy spacing in the meridional direction will resolve most of the meridional velocity signals, even in snapshots like the cruise data. At the same time this spacing is sufficiently far apart that watch circle errors will be small.

Data do not exist to measure the zonal scales of u in this region (the Weisberg and Qiao moorings at 142°W and 138°W would provide some information). We therefore appeal to the physical processes known to influence the zonal currents: the structure of the EUC, the variability introduced by equatorial Kelvin waves, and the variability due to tropical instability waves. Work in the western Pacific during COARE suggests that the zonal pressure gradient and pressure gradient-driven currents spin up in response to wind anomalies on a scale of about 10° longitude (Cronin *et al.*, 2000). Remotely forced equatorial Kelvin waves are dominated by intraseasonal timescales that produce wavelengths of several thousand km. TIW have zonal wavelengths of about 1000 km. Therefore a mooring configuration with zonal separation of 2°–3° should adequately sample the zonal pressure gradient and the zonal current and its derivatives. Results from high-resolution GCMs

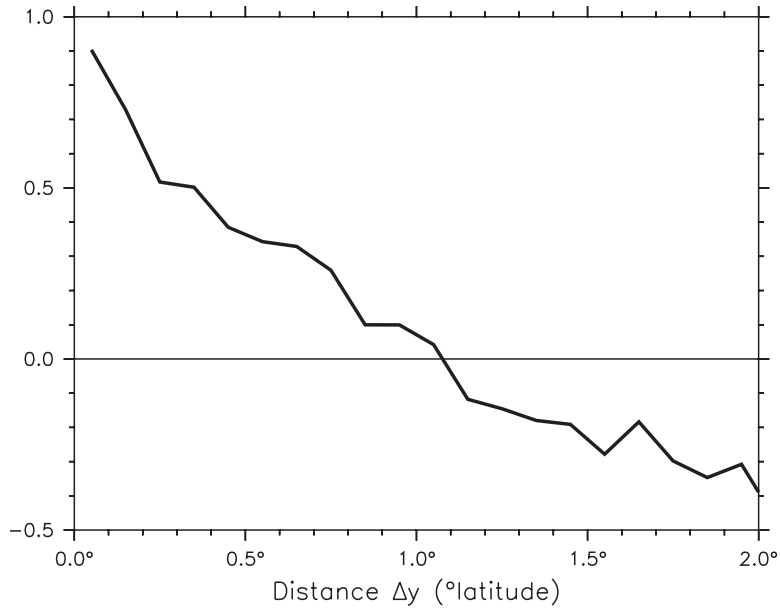

Figure 11: Meridional decorrelation of meridional velocity along 140°W from 2°S to 2°N, measured by shipboard ADCP sections conducted during TAO deployment cruises. The correlation is an average over eight cruises.

will be useful in establishing the appropriate scales for the array (section 3.2.4).

Very-near-surface velocities near the equator in the cold tongue have essentially never been measured. Because of technical limitations (primarily surface reflections), neither shipboard nor present-generation moored ADCP instruments measure velocity within about 20 m of the surface, and estimates of these flows have been based on upward extrapolation of gradients (Weisberg and Qiao, 2000; Johnson *et al.*, 2001). Yet much of the poleward limb of the circulation appears to take place within this extrapolated layer (Fig. 4). A year-long pilot experiment to sample these velocities is underway beginning in May 2004, with point doppler current meters placed at 5, 10, 15, 20 and 25 m on the TAO moorings at 0°, and 2°N, 140°W. In addition a new high-frequency ADCP that will sample velocities from 5–50 m depth with 1 m resolution is being tested at 0°, 140°W at the same time. By the time PUMP is to go in the water the results from these tests will be available to inform the vertical configuration of PUMP moorings.

The two intensive observing periods (see Fig. 13 and section 3.2.3) will offer the opportunity to retrospectively evaluate the adequacy and representativeness of the mooring configurations used. A ship towing a Seasoar will cruise repeatedly across the mooring array, sampling the density and velocity structure at high spatial resolution and nearly synoptic timescale (approximately 12 sections within one month). These data will establish the scales of current variability in the (y,z) plane and allow a quantitative assessment of the errors introduced by the relatively sparse mooring array. The utility of repeated SeaSoar sections in capturing the space and time evolving

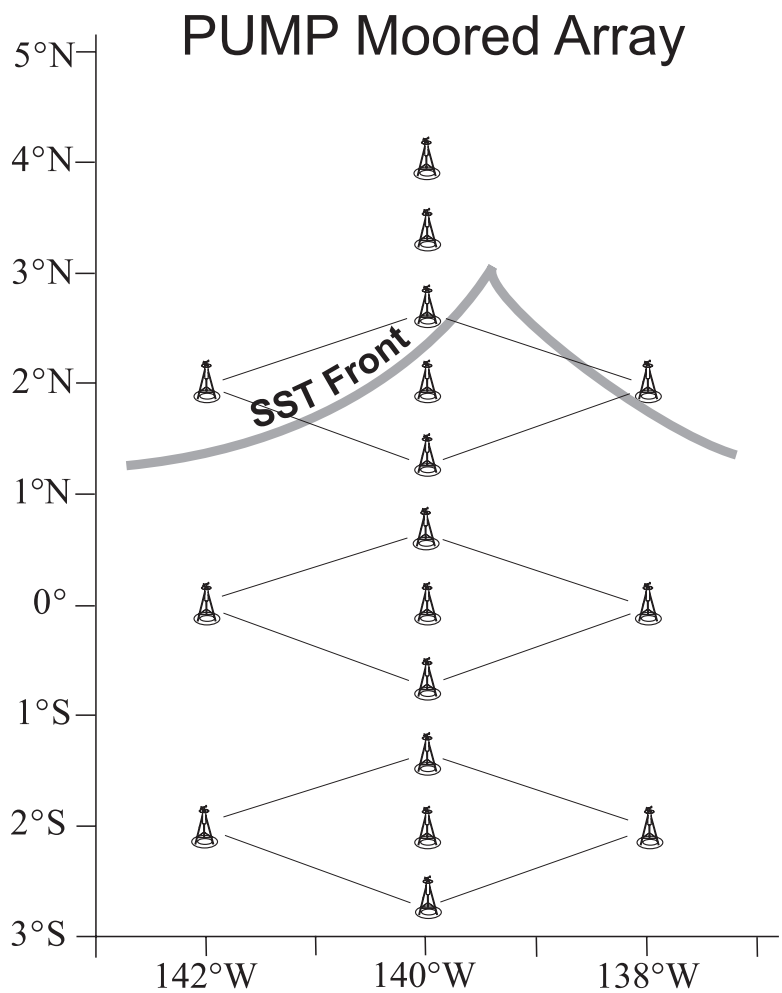

Figure 12: Schematic moored array for PUMP. Each of the 17 moorings pictured is a double-buoy pair, consisting of an enhanced TAO ATLAS (surface) mooring plus a subsurface upward-looking ADCP mooring. The surface moorings are enhanced with point current meters in the upper 20 m to measure the near-surface flows, and with rapid-response thermistors to sample microstructure. Moorings at the center of each diamond are additionally enhanced to measure surface fluxes to enable construction of a heat budget.

structure in the tropical ocean (during COARE) has been demonstrated by Eldin *et al.* (1994) and Richards and Inall (2000).

Gliders can provide fine-scale meridional/vertical structure continuously in parallel with the moorings. The timing of the experiment makes it an excellent candidate for an early intensive use of gliders. A glider deployment will profile from the surface to 500 m over a horizontal distance of 3 km, with a vertical resolution of roughly 5 m. The complete cycle is completed in 3 hours while moving horizontally at about 0.25 m s^{-1}. A single glider takes about one month to complete one section from 3°S to 3°N. Adding more gliders reduces the time taken to occupy one section, and allows more sections. For example, nine gliders would resolve sections at 138°, 140°, and

142°W every 10 days. The gliders need servicing every 6 months, which is reasonably accomplished either from the mooring deployment/recovery cruises, or from the IOP cruises discussed below. The gliders carry combinations of sensors to measure temperature, salinity, pressure, and bio-optical properties. The mounting of an ADCP on a glider is an ongoing development (deployments have already been made) likely to be complete soon.

Glider observations directly address many of the objectives of PUMP by improving on the horizontal resolution of the moorings, while maintaining the same extended temporal coverage. For example, the strength and position of the equatorial front vary on timescales of weeks and longer. Observations during the IOPs, discussed below, will do an excellent job of documenting the meridional/vertical structure of the front and equatorial current system during two single months. The gliders will provide sections, analogous to those from the IOP SeaSoar, every 10 days rather than every 2 days. Thus, the modulation of the equatorial front will be definitively observed, arguably for the first time with adequate spatial resolution. The combination of the gliders' horizontal resolution and the moorings' temporal resolution will undoubtedly provide the most complete sustained description of the equatorial current system ever achieved.

3.2.3 IOPs: Rapid/reduced cooling experiments

Specific Objectives:

- Determine the mechanism(s) by which the generation of internal gravity waves and the resulting turbulent mixing are modulated on diurnal and longer timescales at the equator.
- Determine how this mechanism works off the equator (2°N).
- Determine the spatial structure of mixing across the equatorial region (2°S–4°N).
- Determine the variability of mixing and air-sea forcing across the sharp SST front north of the equator.
- Ultimately, assess the turbulent heat flux integral over a time/space scale that can be meaningfully compared to the heat flux associated with the integrated upwelling.
- Determine the difference in both the nature and magnitude of mixing between the rapid cooling and reduced cooling periods as defined by the annual SST cycle (Fig. 1).

To achieve these objectives, a combination of intensive turbulence profiling both on and off the equator and rapid cross-equatorial surveys of finestructure and mixing are required. These sets of measurements must be coincident and should be repeated at the periods of enhanced cooling and reduced cooling rates (the season of maximum TIW activity). This will require a two-stage process experiment, one to occur in July (Rapid Cooling

Process Experiment) and in November/December (Reduced Cooling Process Experiment). In defining these experiments, we have neglected the heating and steady-state periods. This reflects our bias that upwelling and mixing are reduced during these periods; an inverse calculation by Wang and McPhaden (1999) suggested that vertical mixing at the base of the mixed layer was largest at 140°W during the August–January season. Reduced mixing has been observed in April 1987 (heating phase) and at present we believe it is more crucial to address the periods when it appears that mixing and upwelling significantly alter equatorial SST.

In addition to the intensive surveys, it is highly desirable to also obtain long time series measurements of mixing so that we can both determine the role of mixing in longer term variations than can be resolved with shipborne measurements and evaluate the mixing on the same timescales as the upwelling. For this purpose, development of technology to obtain such observations should be encouraged. Ideally, these time series will be made from the same mooring sites as the divergence and upwelling sampling (section 3.2.2).

Stationary mixing measurements should include turbulence profiling (high sampling rate measurements of temperature, conductivity, and turbulence dissipation) and upper ocean current profiling (acoustic Doppler current profiling). The use of high-frequency echosounders to image the flow may be especially helpful in this flow regime where the combination of high stratification and intense turbulence create the condition for high acoustic backscatter due to small-scale sound speed (density) fluctuations. Modern turbulence profilers include sensors to measure optical backscatter and chlorophyll fluorescence. These also provide estimates of the penetration of incoming solar radiation into the upper ocean, a term that will be critical to any assessment of the vertical profile of net heat flux.

Undulating bodies that are towed (8 kts) whilst profiling from surface to 300 m (e.g., Seasoar) have proven effective at obtaining rapid finescale surveys of in situ properties of the upper water column. Temperature, salinity, and density, as well as optical properties from which the radiative penetration profile can be determined, are pertinent to this aspect of the experiment. Recently, undulating vehicles have been outfitted with scalar microstructure sensors capable of providing a rough estimate of scalar variance dissipation rates (Dillon *et al.*, 2003), which yield an independent estimate of mixing rates. These can be used to clarify the cross-equatorial structure of mixing between and beyond the stationary process mixing ships. Combined with shipboard ADCP sampling, continuous towed body transects across the equator will also help to flesh out the velocity and density features required to assess divergence from moored observations of velocity.

New methods to observe important aspects of the small-scale fluid dynamics (for example, Lagrangian sampling techniques now being tested and deployed) should be encouraged. This is reflected in the strawman budget.

The Process Experiment timeline shown in Fig. 13 indicates a means of obtaining the above objectives. We can expect maximum shipboard durations of 28 d at the equator (assuming 12 d return transit to Honolulu). Mixing ships should be dedicated to obtaining microstructure time series

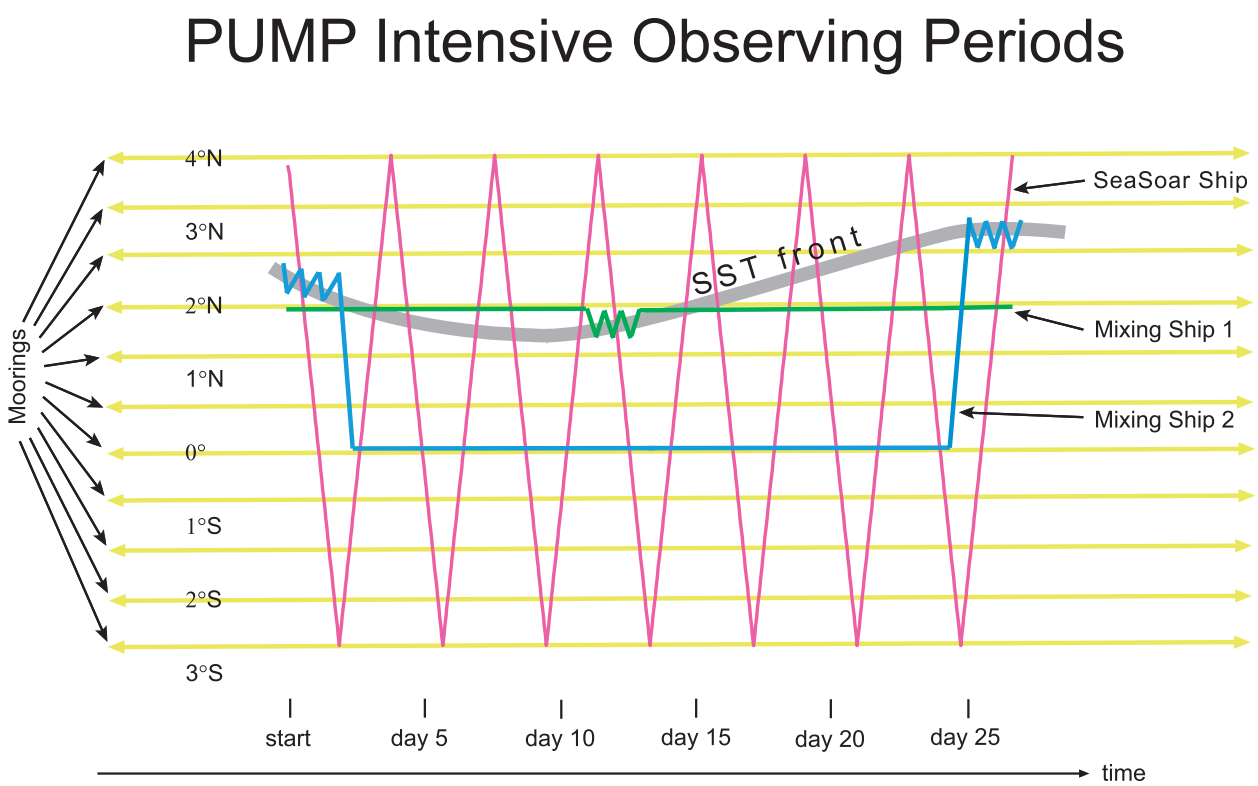

Figure 13: Timeline of PUMP Intensive Observation Periods (two IOPs, during July and November–December). The varying location of the SST front north of the equator is suggested as the grey line. Two sets of intensive mixing observations at 0° and 2°N are made from Mixing Ships (blue, green). These ships will also conduct short intensive surveys across the SST front either on their transit legs or if the front crosses their position (short zigzags). Synoptic cross-equatorial transects are made from the Seasoar ship (red), which can also take atmospheric soundings to study the planetary boundary layer changes across the front. Moorings equipped with sensors to measure microstructure are shown in yellow.

at specific locations (0°, 2°N). However, the effect of the SST front north of the equator may be so influential (especially in the Reduced Cooling period when the instability waves are most active) that we suggest an effort to intensively profile across it as shown in the figure. This profiling will produce a well-defined picture of the front at different phases of the TIW cycle, uniquely embedded in the meso- and large-scale context provided by the mooring line.

The net result of this sampling strategy will include 20+ day time histories of velocity, density, and turbulence fluxes at two locations with synoptic cross-equatorial transects to help define the meridional environment of each. Microstructure time series measurements should be made adjacent to moorings equipped with sensors to measure density, velocity, and mixing. Comparison of the moored observations to the IOP observations will help in interpretation of the longer records. Replication of this sampling strategy should be undertaken in both Rapid Cooling and Reduced Cooling periods.

3.2.4 Modeling

Specific objectives:

- Obtain detailed and computationally exact model heat and momentum budgets for the cold tongue region under a wide variety of conditions, forcing, and modeling choices. Evaluate the errors and uncertainties of budgets estimated from various sampling regimes, including the PUMP Intensive Observing Periods and the sustained broad-scale network.
- Develop metrics for evaluating models. While SST has often been used for model evaluation, compensating errors in surface heat flux and upwelling/mixing can result in SST that is fairly well modeled, despite significant errors in the vertical structure of temperature, salinity, and velocity. Additional metrics might include upper ocean heat content, vertical shear, etc., and careful attention will be paid to their meridional structure, based on the new PUMP sampling.
- Study the sensitivity of simulations and their budgets to different model formulations and resolution. Can we approach convergence?
- Establish the baseline for current state-of-the art modeling of the equatorial cold tongue region. This includes the conventional physical variables of OGCMs plus biogeochemical quantities, the internal wave field, and turbulence in and below the mixed layer. A variety of new models have advanced our abilities in these areas. Understanding their contributions is a first step toward improvement.
- Parameterize the effects of EUC shear and associated internal waves on equatorial mixing in OGCMs. The goal is a functional form that automatically reflects changes in environmental conditions. Use adjoint methodology to systematically study the sensitivity of the equatorial Pacific to parameters in the mixing algorithms.
- Develop and refine parameterizations for deep cycle turbulence beneath the surface mixed layer utilizing the observations from the PUMP field program.
- Develop a data assimilation system to integrate and reconcile the observations collected during the PUMP field program. Ultimately, develop a modeling structure that can use the sustained observing network to infer upwelling and vertical exchanges from broadscale sampling.

To achieve these objectives, the modeling tools will include:

- LES and other fine-scale (DNS) process models for parameterization development.
- High resolution (1–5 km) non-hydrostatic models for parameterization development.

- High resolution (5 km) hydrostatic models for regional simulations of the study area.
- Basin scale OGCM at moderately high resolution (25 km) for testing parameterizations on the basin scale and determine what biases in ocean only simulations still exist.
- Global scale climate component models for application of parameterizations at lower resolution.
- Adjoint and inverse modeling systems for investigation of consistency and diagnosis of parameters.
- Coupled Ocean-Atmosphere GCMs, the final test of the contributions generated by the PUMP program.

Pre-Deployment Planning

A wide variety of models have been recently used to simulate the cold tongue region with increasing resolution and more detailed physics. Evaluation of the gross upper ocean temperature fields in dynamical coupled models shows systematic problems in the mean, the seasonal cycle and the representation of ENSO (Mechoso *et al.*, 1995; Latif *et al.*, 2001; Davey *et al.*, 2002). With the goal of improving the simulation of upwelling and mixing in OGCMs, an essential first step is that an adequate measure be made for the present state of affairs.

The present generation of OGCMs is capable of capturing much of the observed variability of the tropical Pacific, and can be used to make meaningful estimates of the budgets of heat and momentum for the cold tongue region. Most importantly, such estimates may be made under a wide variety of conditions, with varying forcing, model formulations, parameter choices and resolutions (Yu and Schopf, 1997). Such budgets can be computed internally in the model so as to be computationally exact, and can furnish baselines from which observing system simulation studies (OSSEs) can be made. The goal is to evaluate the errors and uncertainties of budgets estimated from various sampling regimes, including the PUMP Intensive Observing Periods and the sustained broad-scale network, using carefully designed regional modeling simulations, so that the uncertainty can be described in terms of sampling error vs. natural variability vs. model ensemble spread, and these can be further distinguished by climate regime (phases of the annual cycle and ENSO). These simulations will also be useful in estimating the spatial scales of density and velocity variability and may lead to adjusting the buoy spacing proposed in section 3.2.2.

Models using data assimilation can be integrated over recent historical periods to ensure that model budgets are evaluated from states consistent with the in situ observational record. These can include the models run for initialization of seasonal forecast systems, such as the NASA GMAO seasonal-to-interannual forecast system, or the SODA analysis. It can also include models utilizing adjoint technology that permits the diagnosis of

parameter sensitivity to control variables. Analysis of historical hindcasts would give information about the mean states and variability of the region, the likelihood of encountering various conditions whether "normal" or anomalous, and establishing a baseline for further experiments after data from the field program has been collected and analyzed.

For such runs, it will be necessary to use high frequency forcing, with winds that reflect the diurnal cycle as well as daily variation. Solar radiation and atmospheric boundary layer conditions must be likewise representative of the high frequency variation inherent to the equatorial Pacific. For the wind fields, satellite scatterometer measurements of the surface stress have been shown to contain important details of the spatial variability of the stress (Chelton *et al.*, 2001), but the temporal resolution of the 2-dimensional fields is insufficient to use this data directly. Some independent description of the statistical nature of the diurnal variation in stress will need to be made.

These models should include various parameterizations of the surface mixed layer and reflect the best and current understanding of how to parameterize mixing in and about the EUC. They should include simulations initialized by data assimilation, as from the NASA NSIPP seasonal prediction system, with simulations made for several months after initialization.

Field Phase Assistance

A regional model of the cold tongue region will be used during the field program to help with the deployment of the ship based observations. The location of the SST front (Fig. 13) is essential for success of the PUMP IOP. While satellite observations can be used directly for identification of SST fronts, data assimilative models can be used to provide the best real-time simulations of the evolving larger scale state of the tropical Pacific. Such models can also be useful as dynamical interpolators for evaluating the representativeness of the shipboard and moored sampling.

Parameterization Development

The challenge in this portion of the work is that in the near term, OGCMs will have resolution on the order of 5 to 10 km at best while the internal waves that are believed to be important in mixing have horizontal scales of less than 1 km. This requires for the foreseeable future that we parameterize the generation of mixing by internal waves as well as the internal waves themselves. At present, it is the mixing that is directly measured by microstructure measurements as well as the internal waves, and parameterizations that have been developed assume that the internal wave spectrum is known. This is the challenge for the development of the parameterizations, which must look beyond the traditional approach of the mixing community to address this scale mismatch. One approach is to use LES simulations.

Parameterization development for GCMs involves the translation of the effects of observed processes operating at very fine spatial scales and with short decorrelation times into suitable algorithms for influencing the large scale state that is simulated within the GCM. This generally involves the

development of an algorithm that describes a set of physical mechanisms that are often best viewed as stochastic. Some of the physical mechanisms of interest will be observed in PUMP on fine spatial scales and with high sampling rates. These observations can best be related to process models operating as large eddy simulations (LES). Such models provide a detailed, physically consistent view of the process, subject to a few, hopefully not too stringent, assumptions that are needed to make the problem tractable. Analysis of the LES simulations in concert with observations will lead to new parameterizations that can be tested in OGCMs (where to DNS fit into this discussion?) where internal waves for the most part do not exist and turbulence is parameterized in simple ways.

An important precedent has been the development of LES models that simulate deep-cycle turbulence (Wang *et al.*, 1998). Large and Gent (1999) have demonstrated that mixing parameterizations can reproduce LES results when careful procedures are used to control for secondary circulations that may arise within the LES studies. This methodology can be extended through the application of the KPP mixing scheme (Large *et al.*, 1994) to high resolution GCM simulations, to explore reasons for the apparent spatial inhomogeneity of deep-cycle turbulence, and provide guidance to both large scale GCMs and future observational programs.

Large Eddy Simulation (LES) can be used to conduct a series of high-resolution simulations of the equatorial boundary layer under the observed range of environmental conditions (especially the variation of EUC vertical shear within 2°S–2°N) to determine the relationship between mixing rate and the environmental conditions. The immediate goal is to assess the extent to which the Ri-schemes used in 1-D models are suitable for varying environmental conditions. Can these schemes be improved by learning from LES results? We emphasize that the goal is a functional form that automatically reflects changes in environmental conditions. Variables other than the Richardson number will likely also need to be included.

An additional objective of the LES modeling would be the momentum fluxes carried by internal gravity waves. These are launched above the EUC core, propagate downward, and break on the lower flank of the EUC. Both local momentum fluxes near the generation site and nonlocal fluxes deeper in the EUC are likely to be important factors determining the evolution of the zonal current system.

LES simulations are not sufficient, however, to fully develop parameterization schemes, and alternative methodologies are sought, especially in the tropical Pacific where wind-driven signals can propagate rapidly into the region in the equatorial wave guide. Thus, horizontally non-local parameterizations may be necessary. Stochastic methods such as those recently studied by Majda and co-workers for the atmosphere (Majda *et al.*, 2003) may well provide a powerful means for developing parameterizations. These methods use stochastic models constrained by the important energetics of the system to arrive at workable coarse-grid algorithms. They draw upon the energetics derived from the LES studies and observations to characterize the fine scale variability.

Sensitivity Studies

Sensitivity testing using the adjoint methodology (Marotzke *et al.*, 1999; Galanti *et al.*, 2002; Galanti and Tziperman, 2003) can be undertaken to systematically study the sensitivity of the equatorial Pacific to unknown or uncertain parameters in mixing parameterizations. More specifically, the sensitivity of the elements that are critical to a correct ENSO simulation, such as the absolute SST over the cold tongue, the strength of the SST gradients in the eastern Pacific, and surface heat fluxes will be examined. In each case, the adjoint method provides the sensitivity of these quantities to unknown and uncertain parameters in the mixing parameterizations used in the model. Examples of such parameters in the KPP mixing scheme are critical Richardson number, background diffusivity, and mixing length. As a result, a quantitative evaluation of what are the critical mixing parameters for a successful simulation can be obtained. In addition, the adjoint can be used to find the sensitivity to these parameters per each geographical location.

Assessment of Model Improvements

Improving global coupled climate models is the key aim of PUMP. Thus a final objective of PUMP will be to include new ocean mixing parameterizations developed during earlier stages of the project into coupled GCMs and examine their impact on coupled climate behavior both for long-term simulations and for seasonal predictions.

The following metrics should be used in assessing performance:

1. Systematic biases in ocean-only simulations. These studies will focus on larger scale and far-field aspects of the improvements accomplished by the new parameterization. The parameterization will also have to be tested to see if it should be applied to regions outside of the cold tongue. Investigation of not only the SST, but also the structure of the currents and whether the thermocline is adequately represented.

2. Biases in coupled ocean-atmosphere GCMs.

3. Error growth in coupled seasonal prediction models.

3.3 Relation with other programs

(a) TAO array

The existence of the TAO array and the availability of its long time series along 140°W is the bedrock foundation for the PUMP experiment. Although the costs and implementation of PUMP (section 3.4) are estimated here independently from TAO, scientifically the projects are closely tied together. The TAO lines east and west of 140°W provide essential context for PUMP, while the enhanced instrumentation

for PUMP is a useful testbed for future TAO enhancements. The information on scales of variability to be developed by PUMP will help to shape the future TAO.

(b) The "Equatorial Box" project

The "Equatorial Box" project is a proposal to NASA to use satellite and in situ data to test and improve models of four key carbon cycle components in the equatorial cold tongue. The PIs (from NASA, NOAA, DOE, and universities) propose to augment the near-surface instrumentation on the TAO mooring lines at 125°W and 140°W, defining a box between those longitudes and 8°S to 8°N. Shallow point current meters are to be placed on each TAO mooring on the two lines at 10 and 20 m depth for estimation of advective terms in the carbon budget. During TAO service cruises, underway sampling from the ships' water intakes, and water sampling on routine CTD profiles, will provide in situ carbon measurements. Additional measurements will be done by pCO_2 samplers on TAO moorings in a parallel NOAA program.

The Equatorial Box project is proposed for the 2005–06 period. If it is funded, these observations will be an excellent lead-in for PUMP, and will provide useful background. Since some of these observations are the same as those we propose, collaboration would be fruitful.

(c) MOTIV (Multiple Observations of Tropical Instability Vortices)

MOTIV is a proposal to NSF and the French space agency CNES to study the physical and biogeochemical conditions of a patch of water circulating within a tropical instability wave vortex near 140°W. Observations will be made during a one-time process study using shipboard instrumentation: ADCPs, mixed layer and subsurface drifting buoys, profiling floats, and a towed SeaSoar platform. The aim is to determine the sources of enhanced productivity in the presence of the TIW vortex. It will address the proposition that eddies influence production through upwelling processes, iron limitation, and eddy pumping.

MOTIV is proposed for 2006. If it is funded, these observations will be complementary to PUMP by providing substantial detail about the evolution of a TIW vortex in the PUMP region.

3.4 Budget and timeline

The purpose of this strawman budget is not to specify precisely what observational techniques are to be used in the PUMP experiment, nor to limit the possibilities. The purpose of listing this instrumentation is to show that the goals of PUMP can be accomplished with existing and field-proven methods, and within a defined budget.

There is also a clear need for new and creative ways to obtain observations of both mixing and upwelling, and to observe other quantities that bear on the objectives of the project. Developments to achieve these should be encouraged. One such targeted observation is long time series of mixing. Another is Lagrangian sampling that would broaden the capabilities beyond the 140°W line targeted here. Others may be equally as important and have escaped the imagination of the authors of this report. Budget placeholders for creative new ways to observe the fields are included in our estimates.

Budget for the 17-mooring, 2-year array shown in Fig. 12:

Each mooring is a tandem pair:

a) Surface buoy with met package, fluxes, T(z) to 500 m, **u**(5,15,25 m), S(1,5,10,25 m)

b) Subsurface upward-looking ADCP buoy

Material costs for the 2-yr array (Including shipping, spares, annual rotation)	\$5.3 m
Personnel costs (PI, operations, lab and seagoing technicians, calibrations)	
(Work ramps up over a total of 4 years)	\$2.8 m
Total cost for 2-yr moored array	**\$8.1 m**

(Subsequent years are relatively inexpensive: Total cost for a 3-yr array = \$9.2 m)

Shiptime required: 40–50 days/year on a Global Class vessel.

Budget for the two intensive observing periods shown in Fig. 13:

5 yr budget estimates for two IOPS plus analysis

Mixing (2 ships, 2 cruises)	\$3.4 m
Seasoar (cruise with technical support from NSF facilities)	\$0.7 m
Gliders (18 gliders)	\$1.0 m
Moored mixing (40 sensors)	\$1.0 m
Placeholder for new techniques to be proposed	\$2.0 m
Total cost for two mixing IOPs	**\$8.1 m**

Shiptime required: 3 Global Class vessels operating simultaneously for two 30-day periods

Budget for historical data analysis: (mostly postdocs) ..... **\$0.5 m**

Budget for the modeling effort described in section 3.2.4:

Survey of existing simulations, development of metrics, budget calculations from present technology (Yr 1, 3–4 groups)	\$0.3 m
High-resolution sensitivity studies, OSSEs (Yr 1–2, 2 groups)	\$0.4 m
LES and DNS simulations (Yr 3–5,2 groups)	\$0.5 m
Parameterization development, testing, validation (Yr 2–5, 3 groups)	\$0.9 m
Field-phase assistance (Yr 3–4, 1 group)	\$0.3 m
Adjoint and inverse modeling (Yr 4–5, 1 group)	\$0.3 m
Equipment, networking	\$0.3 m
Total cost of modeling	**\$3.0 m**

Total budget for experiment as outlined ..... **\$19.7 m**

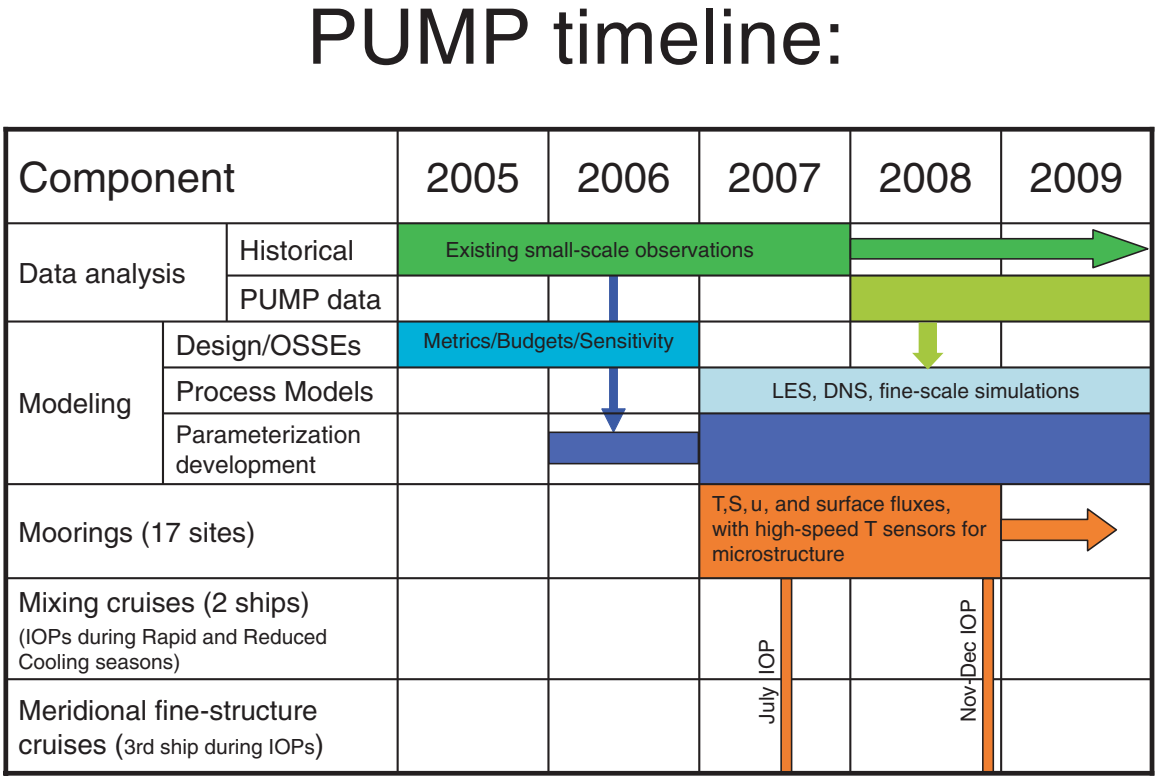

Figure 14: Timeline of PUMP showing the elements described in section 3.2.

4. Acknowledgments

This document benefited greatly from ideas expressed at a workshop in Boulder in May 2003, and from many thoughtful comments on earlier drafts, which broadened the ideas and corrected numerous errors. The enthusiasm shown for this effort, demonstrated in the workshop and in the number of people who took the time to read and criticize this document, encourages us to think that the project will engage a wide community. We gratefully acknowledge the contributions of Dudley Chelton, Eric D'Asaro, Roland deSzoeke, Peter Gent, Mike Gregg, Weiqing Han, Ed Harrison, Bob Helber, Markus Jochum, Eric Johnson, Greg Johnson, Sean Kennan, George Kiladis, Bill Large, Ren-Chieh Lien, John Lyman, Mike McPhaden, Chris Meinen, Dennis Moore, Raghu Murtugudde, Peter Niiler, Clayton Paulson, Kelvin Richards, Dean Roemmich, Pete Strutton, Gabe Vecchi, Dailin Wang and Hemantha Wijesekera.

We thank Ryan Layne Whitney of NOAA/PMEL for the preparation of this document.

References

Barth, J.A., D. Hebert, A.C. Dale, and D.S. Ullman (2004): Direct observations of along-isopycnal upwelling and diapycnal velocity at a shelfbreak front. *J. Phys. Oceanogr.*, *34*, 543–565.

Baturin, N.G., and P.P. Niiler (1997): Effects of instability waves in the mixed layer of the equatorial pacific. *J. Geophys. Res.*, *102*(C13), 27,771–27,793.

Brady, E.C., and H.L. Bryden (1987): Estimating vertical velocity at the equator. *Oceanol. Acta*, *Spec. Vol.*, 33–37.

Bryden, H., and E.C. Brady (1985): Diagnostic model of the three-dimensional circulation in the upper equatorial Pacific Ocean. *J. Phys. Oceanogr.*, *15*, 1255–1273.

Bryden, H., and E.C. Brady (1989): Eddy momentum and heat fluxes and their effects on the circulation of the equatorial Pacific Ocean. *J. Mar. Res.*, *47*, 55–79.

Burns, S.P., D. Khelif, C.A. Freihe, P. Hignett, A.G. Williams, A.L.M. Grant, J.M. Hacker, D.E. Hagan, Y.L. Serra, D.P. Rogers, E.F. Bradley, R.A. Weller, C.W. Fairall, C.A. Paulson, and P.A. Coppin (2000): Comparison of aircraft, ship and buoy radiation and SST measurements from TOGA COARE. *J. Geophys. Res.*, *105*(D12), 15,627–15,652.

Chelton, D.B., S.K. Esbensen, M.G. Schlax, N. Thum, M.H. Freilich, F.J. Wentz, C.L. Gentemann, M.J. McPhaden, and P.S. Schopf (2001): Observations of coupling between surface wind stress and SST in the eastern tropical Pacific. *J. Climate*, *14*(7), 1479–1498.

Cox, M.D. (1980): Generation and propagation of 30-day waves in a numerical model of the Pacific. *J. Phys. Oceanogr.*, *10*, 1168–1186.

Crawford, W.R. (1982): Pacific equatorial turbulence. *J. Phys. Oceanogr.*, *12*(10), 1137–1149.

Crawford, W.R., and T.R. Osborn (1979): Energetics of the Atlantic equatorial undercurrent. *Deep-Sea Res.*, *26*(GATE suppl. II), 309–323.

Crawford, W.R., and T.R. Osborn (1981): Control of equatorial currents by turbulent dissipation. *Science*, *212*, 539–540.

Cromwell, T. (1953): Circulation in a meridional plane in the central equatorial Pacific. *J. Mar. Res.*, *12*, 196–213.

Cronin, M.F., N.A. Bond, C.W. Fairall, and R.A. Well (2004): Surface cloud forcing in the eastern tropical Pacific. In preparation.

Cronin, M.F., and M.J. McPhaden (1997): The upper ocean heat balance in the western equatorial Pacific warm pool during September–December 1992. *J. Geophys. Res.*, *102*, 8533–8553.

Cronin, M.F., M.J. McPhaden, and R.H. Weisberg (2000): Wind forced reversing currents in the western equatorial Pacific. *J. Phys. Oceanogr.*, *30*, 657–676.

Davey, M.K., *et al.* (2002): STOIC: a study of coupled model climatology and variability in tropical ocean regions. *Clim. Dynam.*, *18*, 403–420.

Dillon, T.M., J.A. Barth, A.Y. Erofeev, G.H. May, and H.W. Wijesekera (2003): Microsoar: A new instrument for measuring microscale turbulence from rapidly moving submerged platforms. *J. Atmos. Oceanic Tech.*, *20*, 1671–1684.

Dillon, T.M., J.N. Moum, T.K. Chereskin, and D.R. Caldwell (1989): Zonal momentum balance at the equator. *J. Phys. Oceanogr.*, *19*, 561–570.

Eldin, G., T. Delcroix, C. Henin, K.J. Richards, Y. duPenhoat, J. Picaut, and P. Rual (1994): The large-scale structure of currents and hydrology along 156°e during the COARE intensive observation period. *Geophys. Res. Lett.*, *24*, 2681–2684.

Fairall, C.W., E.F. Bradley, J.E. Hare, A.A. Grachev, and J.B. Edson (2003): Bulk parameterization of air-sea fluxes: Updates and verification for the COARE

algorithm. *J. Climate*, *16*, 571–591.

Fairall, C.W., E.F. Bradley, D.P. Rogers, J.B. Edson, and G.S. Young (1996): Bulk parameterization of air-sea fluxes for the Tropical Ocean/Global Atmosphere—Coupled Ocean Atmosphere Response Experiment. *J. Geophys. Res.*, *101*, 3747–3764.

Feng, M., P. Hacker, and R. Lukas (1998): Upper ocean heat and salt balances in response to a westerly wind burst in the western equatorial Pacific during TOGA COARE. *J. Geophys. Res.*, *103*(C5), 10,289–10,311.

Feng, M., R. Lukas, P. Hacker, R.A. Weller, and S.P. Anderson (2000): Upper ocean heat and salt balances in the western equatorial Pacific in response to the intraseasonal oscillation during TOGA COARE. *J. Climate*, *13*, 2409–2427.

Flament, P.J., S.C. Kennan, R.A. Knox, P.P. Niiler, and R.L. Bernstein (1996): The three-dimensional structure of an upper ocean vortex in the tropical Pacific Ocean. *Nature*, *383*, 610–613.

Galanti, E., and E. Tziperman (2003): A midlatitude-ENSO teleconnection mechanism via baroclinically unstable Rossby waves. *J. Phys. Oceanogr.*, *33*, 1877–1888.

Galanti, E., E. Tziperman, M. Harrison, A. Rosati, R. Giering, and Z. Sirkes (2002): The equatorial thermocline outcropping—A seasonal control on the tropical Pacific Ocean-atmosphere instability strength. *J. Climate*, *15*, 2721–2739.

Godfrey, J.S., R.A. Houze, R.H. Johnson, R. Lukas, J.-L. Redelsperger, A. Sumi, and R. Weller (1998): Coupled Ocean-Atmosphere Response Experiment (COARE): An interim report. *J. Geophys. Res.*, *103*, 14,395–14,450.

Gregg, M.C. (1976): Temperature and salinity microstructure in the equatorial undercurrent. *J. Geophys. Res.*, *81*, 1180–1196.

Gregg, M.C., H. Peters, J. Wesson, N. Oakey, and T. Shay (1985): Intensive measurements of turbulence and shear in the equatorial undercurrent. *Nature*, *318*, 140–144.

Halpern, D., and H.P. Freitag (1987): Vertical motion in the upper ocean of the equatorial Pacific. *Oceanol. Acta*, *Spec. Vol.*, 19–26.

Halpern, D., R.A. Knox, and D.S. Luther (1988): Observations of 20-day period meridional current oscillations in the upper ocean along the Pacific equator. *J. Phys. Oceanogr.*, *18*, 1514–1534.

Hansen, D.V., and C.A. Paul (1987): Vertical motion in the eastern equatorial Pacific inferred from drifting buoys. *Oceanol. Acta*, *Spec. Vol.*, 27–32.

Hazeleger, W., P. De Vries, and Y. Friocourt (2003): Sources of the equatorial undercurrent in a high-resolution ocean model. *J. Phys. Oceanogr.*, *33*.

Hebert, D., J.N. Moum, and D.R. Caldwell (1991): Does ocean turbulence peak at the equator? Revisited. *J. Phys. Oceanogr.*, *21*, 1690–1698.

Jochum, M., P. Malanotte-Rizzoli, and A. Busalacchi (2004): Tropical instability waves in the Atlantic Ocean. *Ocean Modelling*, *7*, 145–163.

Johnson, E.S., and D.S. Luther (1994): Mean zonal momentum balance in the upper and central equatorial Pacific Ocean. *J. Geophys. Res.*, *99*, 7689–7705.

Johnson, G.C. (2001): The Pacific Ocean subtropical cell surface limb. *Geophys. Res. Lett.*, *28*, 1771–1774.

Johnson, G.C., M.J. McPhaden, and E. Firing (2001): Equatorial Pacific horizontal velocity, divergence and upwelling. *J. Phys. Oceanogr.*, *31*, 839–849.

Johnson, G.C., B.M. Sloyan, W.S. Kessler, and K.E. McTaggart (2002): Direct measurements of upper ocean currents and water properties across the tropical Pacific during the 1990s. *Prog. Oceanogr.*, *52*, 31–61.

Kessler, W.S., L.M. Rothstein, and D. Chen (1998): The annual cycle of SST in the eastern tropical Pacific, diagnosed in an ocean GCM. *J. Climate*, *11*, 777–799.

Knauss, J.A. (1963): Equatorial current systems. In *The Sea*, Wiley-Interscience, 235–252.

Large, W.G., and P.R. Gent (1999): Validation of vertical mixing in an equatorial ocean model using large eddy simulations and observations. *J. Phys. Oceanogr.*, *29*, 449–464.

Large, W.G., J.C. McWilliams, and S.C. Doney (1994): Oceanic vertical mixing—a review and a model with a nonlocal boundary layer parameterization. *Rev. Geophys.*, *32*, 363–403.

Latif, M., *et al.* (2001): ENSIP: the El Niño intercomparison project. *Clim. Dynam.*, *18*, 255–276.

Ledwell, J.R., A.J. Watson, and C.S. Law (1995): Evidence for slow mixing across the pycnocline from an open-ocean tracer-release experiment. *Nature*, *364*, 701=703.

Legeckis, R. (1977): Long waves in the eastern equatorial Pacific Ocean: A view from geostationary satellite. *Science*, *197*(4309), 1179–1181.

Lien, R.C., E.A. D'Asaro, and M.J. McPhaden (2002): Internal waves and turbulence in the upper central equatorial Pacific: Lagrangian and Eulerian observations. *J. Geophys. Res.*, *32*, 2619–2639.

Lien, R.S., D.R. Caldwell, M.C. Gregg, and J.N. Moum (1995): Turbulence variability at the equator in the central Pacific at the beginning of the 1991–1993 El Niño. *J. Geophys. Res.*, *100*, 6881–6898.

Lu, P., J.P. McCreary, and B.A. Klinger (1998): Meridional circulation cells and the source waters of the Pacific equatorial undercurrent. *J. Phys. Oceanogr.*, *28*, 62–84.

Luther, D.S., and E.S. Johnson (1990): Eddy energetics in the upper equatorial Pacific during the Hawaii-to-Tahiti Shuttle Experiment. *J. Phys. Oceanogr.*, *20*, 913–944.

Lyman, J.M., G.C. Johnson, and W.S. Kessler (2004): Structure of 17-day versus 33-day tropical instability waves in the equatorial Pacific. *J. Phys. Oceanogr.*, submitted.

Mack, A.P., and D. Hebert (1997): Internal gravity waves in the upper eastern equatorial Pacific: observations and numerical solutions. *J. Geophys. Res.*, *102*, 21,081–21,100.

Majda, A.J., I. Timofeyev, and E. Vanden-Eijden (2003): Systematic strategies for stochastic mode reduction in climate. *J. Atmos. Sci.*, *60*, 1705–1722.

Marotzke, J., R. Giering, K.Q. Zhang, D. Stammer, C. Hill, and T. Lee (1999): Construction of the adjoint MIT ocean general circulation model and application to atlantic heat transport sensitivity. *J. Geophys. Res.*, *104*(C12), 29,529–29,547.

Masina, S., and S.G.H. Philander (1999): An analysis of tropical instability waves in a numerical model of the Pacific Ocean—1. Spatial variability of the waves. *J. Geophys. Res.*, *104*(C12), 29,613–29,635.

Masina, S., S.G.H. Philander, and A.B.G. Bush (1999): An analysis of tropical instability waves in a numerical model of the Pacific Ocean, 2, Generation and energetics of the waves. *J. Geophys. Res.*, *104*(C12), 29,637–29,661.

McCreary, J.P., and P. Lu (1994): Interaction between the subtropical and equatorial ocean circulations—The subtropical cell. *J. Phys. Oceanogr.*, *24*, 466–497.

McPhaden, M.J. (1981): Continuously stratified models of the steady-state equatorial ocean. *J. Phys. Oceanogr.*, *11*, 337–354.

McPhaden, M.J. (1993): TOGA-TAO and the 1991–93 El Niño-Southern Oscillation event. *Oceanography*, *6*, 36–44.

McPhaden, M.J. (1996): Monthly period oscillations in the Pacific North Equatorial Countercurrent. *J. Geophys. Res.*, *101*, 6337–6360.

McPhaden, M.J. (1999): Genesis and evolution of the 1997–98 El Niño. *Science*, *283*, 950–954.

McPhaden, M.J., and H. Peters (1992): Diurnal cycle of internal wave variability in the equatorial Pacific Ocean: results from moored observations. *J. Phys.*

Oceanogr., *22*, 1317–1329.

Mechoso, C.R., A.W. Robertson, J.D. Neelin, N. Barth, M.K. Davey, S. Ineson, P. Delecluse, P.R. Gent, J.J. Tribbia, B. Kirtman, M. Latif, H. Le Treut, J. Polcher, T. Nagai, S.G.H. Philander, P.S. Schopf, M.J. Suarez, T. Stockdale, L. Terray, and O. Thual (1995): The seasonal cycle over the tropical Pacific in coupled ocean-atmosphere general circulation models. *Mon. Weather Rev.*, *123*, 2825–2838.

Meehl, G.A., P.R. Gent, J.M. Arblaster, B.L. Otto-Bliesner, E.C. Brady, and A. Craig (2001): Factors that affect the amplitude of El Niño in global coupled climate models. *Clim. Dynam.*, *17*, 515–526.

Meinen, C.S., M.J. McPhaden, and G.C. Johnson (2001): Vertical velocities and transports in the equatorial Pacific during 1993–99. *J. Phys. Oceanogr.*, *31*, 3230–3248.

Moum, J.N., and D.R. Caldwell (1985): Local influences on shear-flow turbulence in the equatorial ocean. *Science*, *230*, 315–316.

Moum, J.N., D.R. Caldwell, and C.A. Paulson (1989): Mixing in the equatorial surface layer and thermocline. *J. Geophys. Res.*, *94*, 2005–2021.

Moum, J.N., D.R. Caldwell, C.A. Paulson, T.K. Cheresin, and L.A. Regier (1986): Does ocean turbulence peak at the equator? *J. Phys. Oceanogr.*, *16*, 1991–1994.

Moum, J.N., M.C. Gregg, R.C. Lien, and M.E. Carr (1995): Comparison of turbulence kinetic energy dissipation rate estimates from two ocean microstructure profilers. *J. Atmos. Oceanic Tech.*, *12*, 346–366.

Moum, J.N., D. Hebert, C.A. Paulson, and D.R. Caldwell (1992): Turbulence and internal waves at the equator. Part 1: Statistics from towed thermistors and a microstructure profiler. *J. Phys. Oceanogr.*, *22*, 1330–1345.

Murtugudde, R., J. Beauchamp, and A.J. Busalacchi (2002): Effects of penetrative radiation on the upper tropical ocean circulation. *J. Climate*, *15*, 470–486.

Nakamoto, S., S. Prasanna Kumar, J.M. Oberhuber, J. Ishizaka, K. Muneyama, and R. Frouin (2001): Response of the equatorial Pacific to chlorophyll pigment in a mixed layer isopycnal ocean general circulation model. *Geophys. Res. Lett.*, *28*, 2021–2024.

Neelin, J.D., D.S. Battisti, F.-F.J. A. C. Hirst, Y. Wakata, T. Yamagata, and S.E. Zebiak (1998): ENSO theory. *J. Geophys. Res.*, *103*(C7), 14,261–14,290.

Ohlmann, J.C. (2003): Ocean radiant heating in climate models. *J. Climate*, *16*, 1337–1351.

Osborn, T.R., and L.E. Bilodeau (1980): Temperature microstructure measurements in the equatorial Atlantic. *J. Phys. Oceanogr.*, *10*, 66–82.

Peters, H., M.C. Gregg, and T. Sanford (1991): Equatorial and off-equatorial fine-scale and large-scale shear variability at 140°W. *J. Geophys. Res.*, *96*, 16,913–16,928.

Peters, H., M.C. Gregg, and J.M. Toole (1988): On the parameterization of equatorial turbulence. *J. Geophys. Res.*, *93*, 1199–1218.

Philander, S.G.H. (1976): Instabilities of zonal equatorial currents. *J. Geophys. Res.*, *81*, 3725–3735.

Philander, S.G.H. (1978): Instabilities of zonal equatorial currents, 2. *J. Geophys. Res.*, *83*, 3779–3782.

Poulain, P.-M. (1993): Estimates of horizontal divergence and vertical velocity in the equatorial Pacific. *J. Phys. Oceanogr.*, *23*, 601–607.

Qiao, L., and R.H. Weisberg (1998): Tropical instability waves energetics: Observations from the Tropical Instability Wave Experiment. *J. Phys. Oceanogr.*, *28*, 345–360.

Raymond, D.J., S.K. Esbensen, M. Gregg, and C.S. Bretherton (2004): EPIC2001 and the coupled ocean-atmosphere system of the tropical east Pacific. *Bull. Am. Meteorol. Soc.*, submitted.

Richards, K.J., and M.E. Inall (2000): The upper ocean heat content of the western equatorial Pacific: Processes controlling its exchange during TOGA-COARE. *J. Geophys. Res.*, *105*, 19,575–19,590.

Rossow, W.B., and Y.C. Zhang (1995): Calculation of surface and top of atmosphere radiative fluxes from physical quantities based on ISCCP data sets. 2. Validation and first results. *J. Geophys. Res.*, *100*(D1), 1167–1197.

Rudnick, D.L. (1996): Intensive surveys of the Azores Front, 2, Inferring the geostrophic and vertical velocity fields. *J. Geophys. Res.*, *101*, 16,291–16,303.

Smyth, W.D., D. Hebert, and J.N. Moum (1996): Oceanic response to a westerly wind burst, Part II: Thermal and freshwater responses. *J. Geophys. Res.*, *101*, 22,513–22,534.

Smyth, W.D., and J.N. Moum (2002): Waves and instability in an asymmetrically stratified jet. *Dynam. Atmos. Ocean*, *35*, 265–294.

Strutton, P.G., and F.P. Chavez (2004): Biological heating in the equatorial Pacific: Observed variability and potential for real-time calculation. *J. Climate*, *17*, 1097–1109.

Sun, C., W.D. Smyth, and J.N. Moum (1998): Dynamic instability of stratified shear flow in the upper equatorial Pacific. *J. Geophys. Res.*, *103*, 10,323–10,337.

Sutherland, B.R. (1996): Dynamic excitation of internal gravity waves in the equatorial oceans. *J. Phys. Oceanogr.*, *26*, 2398–2419.

Swenson, M.S., and D.V. Hansen (1999): Tropical Pacific Ocean mixed layer heat budget: The Pacific cold tongue. *J. Phys. Oceanogr.*, *29*, 69–81.

Wang, Q., J.C. McWilliams, and W.G. Large (1998): Large-eddy simulation of the diurnal cycle of deep equatorial turbulence. *J. Phys. Oceanogr.*, *28*, 129–148.

Wang, W., and M.J. McPhaden (1999): The surface-layer heat balance in the equatorial Pacific Ocean. Part I: Mean seasonal cycle. *J. Phys. Oceanogr.*, *29*, 1812–1831.

Wang, W., and M.J. McPhaden (2001): Surface layer temperature balance in the equatorial Pacific during the 1997–98 El Niño and the 1998–99 La Niña. *J. Climate*, *14*, 3393–3407.

Weidman, P.D., D.L. Mickler, B. Dayyani, and G.H. Born (1999): Analysis of Legeckis eddies in the near-equatorial Pacific. *J. Geophys. Res.*, *104*, 7865–7887.

Weisberg, R.H., and L. Qiao (2000): Equatorial upwelling in the central Pacific estimated from moored velocity profilers. *J. Phys. Oceanogr.*, *30*, 105–124.

Weller, R.A., and S.P. Anderson (1996): Surface meteorology and air-sea fluxes in the western equatorial Pacific warm pool during the TOGA Coupled Ocean-Atmosphere Response Experiment. *J. Climate*, *9*, 1959–1990.

Wijesekera, H., and T.M. Dillon (1991): Internal waves and mixing in the upper equatorial Pacific Ocean. *J. Geophys. Res.*, *96*, 7115–7125.

Wyrtki, K. (1981): An estimate of equatorial upwelling in the Pacific. *J. Phys. Oceanogr.*, *11*, 1205–1214.

Yoder, J.A., S.G. Ackleson, R.T. Barber, P. Flament, and W.M. Balch (1994): A line in the sea. *Nature*, *371*, 689–692.

Yu, L.S., R.A. Weller, and B.M. Sun (2004): Improving latent and sensible heat flux estimates for the Atlantic Ocean (1988–99) by a synthesis approach. *J. Climate*, *17*, 373–393.

Yu, Z.J., J.P. McCreary, and J.A. Proehl (1995): Meridional asymmetry and energetics of tropical instability waves. *J. Phys. Oceanogr.*, *25*(12), 2997–3007.

Yu, Z.J., and P.S. Schopf (1997): Vertical eddy mixing in the tropical upper ocean: Its influence of zonal currents. *J. Phys. Oceanogr.*, *27*, 1447–1458.